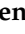



## Article

# Obesity and Environmental Risk Factors Significantly Modify the Association between Ischemic Stroke and the Hero Chaperone *C19orf53*

Irina Shilenok<sup>1,2</sup>, Ksenia Kobzeva<sup>1</sup> , Alexey Deykin<sup>3,4</sup>, Vladimir Pokrovsky<sup>5</sup>, Evgeny Patrakhanov<sup>5</sup> and Olga Bushueva<sup>1,6,\*</sup> 

- <sup>1</sup> Laboratory of Genomic Research, Research Institute for Genetic and Molecular Epidemiology, Kursk State Medical University, 305041 Kursk, Russia
- <sup>2</sup> Division of Neurology, Kursk Emergency Hospital, 305035 Kursk, Russia
- <sup>3</sup> Laboratory of Genome Editing for Biomedicine and Animal Health, Belgorod State National Research University, 308015 Belgorod, Russia
- <sup>4</sup> Department of Pharmacology and Clinical Pharmacology, Belgorod State National Research University, 308015 Belgorod, Russia
- <sup>5</sup> Laboratory of Genetic Technologies and Gene Editing for Biomedicine and Veterinary Medicine, Belgorod State National Research University, 308015 Belgorod, Russia
- <sup>6</sup> Department of Biology, Medical Genetics and Ecology, Kursk State Medical University, 305041 Kursk, Russia
- \* Correspondence: olga.bushueva@inbox.ru

**Abstract:** The unique chaperone-like properties of *C19orf53*, discovered in 2020 as a “hero” protein, make it an intriguing subject for research in relation to ischemic stroke (IS). Our pilot study aimed to investigate whether *C19orf53* SNPs are associated with IS. DNA samples from 2138 Russian subjects (947 IS and 1308 controls) were genotyped for 7 *C19orf53* SNPs using probe-based PCR. Dominant (D), recessive (R), and log-additive (A) regression models in relation to the effect alleles (EA) were used to interpret associations. An increased risk of IS was associated with rs10104 (EA G;  $P_{\text{bonf(R)}} = 0.0009$ ;  $P_{\text{bonf(A)}} = 0.0004$ ), rs11666524 (EA A;  $P_{\text{bonf(R)}} = 0.003$ ;  $P_{\text{bonf(A)}} = 0.02$ ), rs346158 (EA C;  $P_{\text{bonf(R)}} = 0.006$ ;  $P_{\text{bonf(A)}} = 0.045$ ), and rs2277947 (EA A;  $P_{\text{bonf(R)}} = 0.002$ ;  $P_{\text{bonf(A)}} = 0.01$ ) in patients with obesity; with rs11666524 (EA A;  $P_{\text{bonf(R)}} = 0.02$ ), rs346157 (EA G;  $P_{\text{bonf(R)}} = 0.036$ ), rs346158 (EA C;  $P_{\text{bonf(R)}} = 0.005$ ), and rs2277947 (EA A;  $P_{\text{bonf(R)}} = 0.02$ ) in patients with low fruit and vegetable intake; and with rs10104 (EA G;  $P_{\text{bonf(R)}} = 0.03$ ) and rs11666524 (EA A;  $P_{\text{bonf(R)}} = 0.048$ ) in patients with low physical activity. In conclusion, our pilot study provides comprehensive genetic and bioinformatic evidence of the involvement of *C19orf53* in IS risk.

**Keywords:** *C19orf53*; chromosome 19 open reading frame 53; SNP; obesity; low fruit and vegetable intake; low physical activity; chaperones; heat-resistant obscure; hero; ischemic stroke



**Citation:** Shilenok, I.; Kobzeva, K.; Deykin, A.; Pokrovsky, V.; Patrakhanov, E.; Bushueva, O. Obesity and Environmental Risk Factors Significantly Modify the Association between Ischemic Stroke and the Hero Chaperone *C19orf53*. *Life* **2024**, *14*, 1158. <https://doi.org/10.3390/life14091158>

Academic Editors: Irina-Iuliana Costache and Minerva Codruta Badescu

Received: 31 July 2024

Revised: 7 September 2024

Accepted: 10 September 2024

Published: 12 September 2024



**Copyright:** © 2024 by the authors. Licensee MDPI, Basel, Switzerland. This article is an open access article distributed under the terms and conditions of the Creative Commons Attribution (CC BY) license (<https://creativecommons.org/licenses/by/4.0/>).

## 1. Introduction

An ischemic stroke (IS) is recognized as a major contributor to morbidity and mortality worldwide [1]. An IS is a localized brain injury resulting from a substantial decrease in cerebral blood flow within major cerebral arteries caused by embolism or thrombosis usually following atherosclerotic plaque rupture [2]. Acute ischemia leads to cell death directly via severe metabolic deficits or via secondary alteration as a result of inflammation and blood–brain barrier opening [3].

A crucial mechanism in minimizing cellular damage in an ischemia–reperfusion injury involves the utilization of chaperone machinery [4,5]. Chaperones form a functionally linked network of proteins dedicated to ensuring the quality of proteome—a pivotal process for cellular protection against lethal stress [6,7]. Moreover, chaperones have been implicated in a wide range of processes markedly important for IS etiology, such as vascular

tone regulation [8–10], atherosclerotic plaque formation and dynamics [11–13], and platelet aggregation [14,15].

C19orf53, also known as Chromosome 19 Open Reading Frame 53, plays a role in mediating excessive cell proliferation, leading to metabolic imbalance and increased oxidative stress in response to toxins [16]. Associated with various biological pathways, including rRNA biogenesis, ovarian cancer, and Zika virus replication [17,18], C19orf53 gained attention in 2020 when Tsuboyama K et al. identified it along with other small heat-resistant proteins displaying chaperone-like activity in cell culture lysate [19]. Referred to as “heat-resistant obscure” or “Hero”, C19orf53 exhibited resilience, emphasizing its chaperone-like characteristics. Given the significance of chaperones in IS, exploring the newfound properties of C19orf53 protein is crucial for understanding its potential implications in the disease. All Hero genes previously studied by us showed significant associations with the risk of developing an IS [20–22], suggesting their potentially significant role in the molecular mechanisms of IS development, most likely due to their pronounced chaperone-like properties. In addition, a recent study has established the role of C19orf53 in suppressing the pathological aggregation of TAR DNA-binding protein 43, which plays an important role in neurodegenerative diseases [23]. Given the significance of chaperones in IS, exploring the newfound properties of C19orf53 protein is crucial for understanding its potential implications in the disease.

The aim of our study was to investigate whether the polymorphism of the *C19orf53* gene, encoding a heat-resistant obscure (Hero) protein with chaperone-like activity, is associated with the risk and clinical features of ischemic stroke.

## 2. Materials and Methods

The outline of the study design is shown in Figure 1.

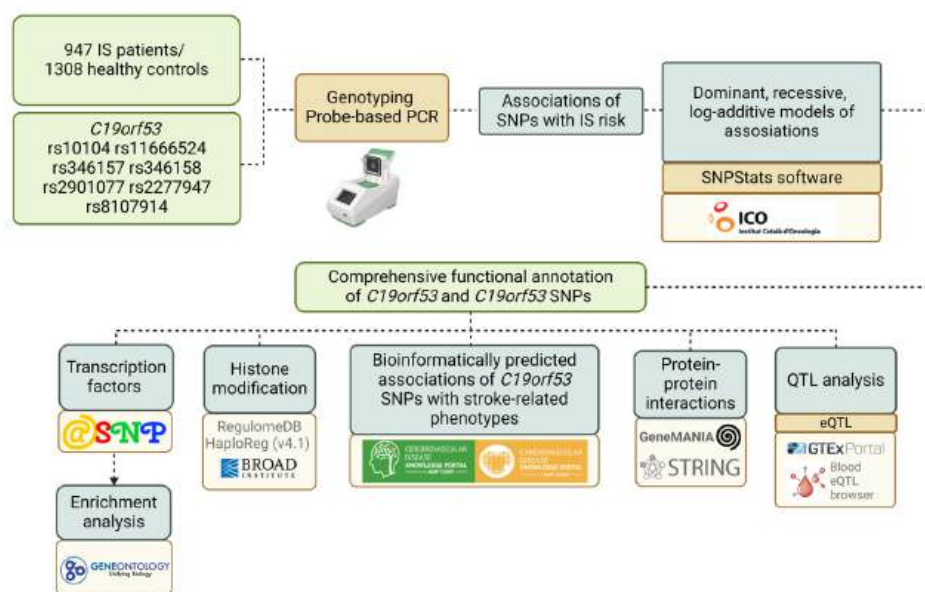


**Figure 1.** The outline of the study design.

### 2.1. Experimental Design

The study included 2138 unrelated individuals from central Russia, comprising 947 IS patients and 1308 healthy individuals. The Ethical Review Committee of Kursk State Medical University approved the study protocol, and all participants provided written informed consent. Inclusion criteria for the study required participants to have self-declared Russian ancestry and to be born in central Russia.

Table 1 provides general clinical characteristics of IS patients and controls.

**Table 1.** General clinical characteristics of IS patients and controls.

Baseline and Clinical Characteristics		IS Patients (n = 947)	Controls (n = 1308)	p-Value
	Age, Me [Q1; Q3]	63 [55; 70]	59 [53; 66]	<b>&lt;0.001</b>
Gender	Males, N (%)	524 (55.33%)	614 (46.9%)	<b>&lt;0.001</b>
	Females, N (%)	423 (44.67%)	694 (53.1%)	
Smoking	Yes, N (%)	469 (49.52%)	413 (31.6%)	<b>&lt;0.001</b>
	No, N (%)	478 (50.48%)	895 (68.4%)	
Low physical activity	Yes, N (%)	354 (39.91%)	ND	
	No, N (%)	533 (60.09%)		
Low fruit/vegetable consumption	Yes, N (%)	416 (46.9%)	ND	
	No, N (%)	471 (53.1%)		
Coronary artery disease	Yes, N (%)	116 (13.08%)	-	
	No, N (%)	771 (86.92%)	-	
Obesity	Yes, N (%)	61 (6.4%)	ND	
	No, N (%)	530 (56%)		
	ND, N (%)	356 (37.6%)		
Family history of cerebrovascular diseases	Yes, N (%)	312 (35.29%)	ND	
	No, N (%)	572 (64.71%)	ND	
	Age at onset of stroke, Me [Q1; Q3]	61 [54; 70] (n = 904)	-	
Number of strokes including event in question	1, N (%)	800 (88.59%)	-	
	2, N (%)	89 (9.86%)	-	
	3, N (%)	14 (1.55%)	-	
Stroke localization	Right/left middle cerebral artery basin, N (%)	750 (83.24%)	-	
	Vertebrobasilar basin, N (%)	151 (16.76%)	-	
	Area of lesion in stroke, mm <sup>2</sup> , Me [Q1; Q3]	105 [30; 468] (n = 883)	-	
	Total cholesterol, mmol/L, Me [Q1; Q3]	5.2 [4.4; 5.9] (n = 608)	ND	
	Triglycerides, mmol/L, Me [Q1; Q3]	1.3 [1.1; 1.8] (n = 601)	ND	
	Glucose level, mmol/L, Me [Q1; Q3]	4.8 [4.3; 5.5] (n = 892)	ND	
	Prothrombin time, seconds, Me [Q1; Q3]	10.79 [10.14; 11.70] (n = 880)	ND	
	International normalized ratio, Me [Q1; Q3]	1 [0.94; 1.09] (n = 596)	ND	
	Activated partial thromboplastin time, seconds, Me [Q1; Q3]	32.7 [29; 37] (n = 599)	ND	

Statistically significant differences between groups are indicated in bold; ND—no data.

The patients were enrolled in the study during two distinct periods: from 2015 to 2017 at the Regional Vascular Center of Kursk Regional Clinical Hospital [24,25] and from 2010 to 2012 at the Neurology Clinics of Kursk Emergency Medicine Hospital [26,27].

Inclusion criteria for the study required patients to have a diagnosis of ischemic stroke, confirmed by neurologists during the acute phase of the disease based on clinical and neurological evaluations and verified by computed tomography or magnetic resonance imaging of the brain performed within the first 48 hours following the stroke event. The study included the following subtypes of ischemic stroke: atherothrombotic, cardioembolic, and stroke of unknown etiology. Exclusion criteria included patients with liver or kidney failure, endocrine, autoimmune, oncological, or other conditions that could lead to an acute cerebrovascular accident. Additionally, patients with hemorrhagic stroke, secondary intracerebral hemorrhage, hemodynamic, hemorheological, or dissection stroke as well as those with traumatic brain injury were excluded. All included IS patients had a documented history of hypertension and were receiving antihypertensive treatment.

The control group consisted of healthy volunteers who had normal blood pressure, did not receive antihypertensive therapy, and showed no clinical symptoms of cardiovascular, cerebrovascular, or other significant illnesses. Healthy individuals were included in the control group if their systolic blood pressure was below 130 mm Hg and diastolic blood pressure was below 85 mm Hg, based on at least three separate measurements. Controls from the Kursk region were selected from hospitals during routine medical examinations conducted in public institutions and industrial establishments. This group was recruited from the same population and during the same time period.

In accordance with WHO guidelines, low fruit and vegetable consumption was defined as consuming less than 400 g per day. Adequate consumption of fresh vegetables and fruits was defined as consuming 400 g or more, equivalent to 3–4 servings per day, excluding starchy tubers like potatoes.

The following criteria were used to choose the SNPs: have a minor allele frequency of at least 0.05 in the European population and be distinguished by a high regulatory potential.

The bioinformatic tools LD TAG SNP Selection (TagSNP) and SNPinfo Web Server (<https://snpinfo.niehs.nih.gov/> (accessed on 15 March 2022)) were utilized to choose SNPs based on the reference haplotypic structure of the Caucasian population (CEU) of the project HapMap. The *C19orf53* (Chromosome 19 Open Reading Frame 53, ID: 26135) gene contains seven SNPs (rs10104, rs11666524, rs346157, rs346158, rs2901077, rs2277947, and rs8107914). SNP rs10104 is a missense variant, SNPs rs11666524, rs346157, rs346158, rs2901077 are located in introns, and SNPs rs2277947 and rs8107914 are located in the 3 prime UTRs.

## 2.2. Genetic Analysis

Genotyping was carried out by the Laboratory of Genomic Research at the Research Institute for Genetic and Molecular Epidemiology. Venous blood samples (up to 5 mL) were drawn from each participant's cubital vein and placed in EDTA-coated tubes, which were then stored at  $-20^{\circ}\text{C}$  until processing. Genomic DNA was extracted from the thawed blood samples using standard phenol/chloroform extraction and ethanol precipitation methods. The purity, quality, and concentration of the extracted DNA were evaluated using a NanoDrop spectrophotometer (Thermo Fisher Scientific, Waltham, MA, USA).

Detection of SNP variations in the *C19orf53* gene was conducted using Taq-Man-based PCR following protocols developed at the Research Institute for Genetic and Molecular Epidemiology. Primer design was carried out using Primer3 software version 4.1.0 [28], with the specific primers and probes listed in Table S1. The real-time PCR was performed in a 25  $\mu\text{L}$  reaction mixture containing 1.5 units of Hot Start Taq DNA polymerase (Biolabmix, Novosibirsk, Russia), approximately 10 ng of DNA, and the following reagent concentrations: 0.25  $\mu\text{M}$  of each primer; 0.1  $\mu\text{M}$  of each probe; 250  $\mu\text{M}$  of each dNTP; 2.5 mM  $\text{MgCl}_2$ ; 1 $\times$ PCR buffer (67 mM Tris-HCl, pH 8.8, 16.6 mM  $(\text{NH}_4)_2\text{SO}_4$ , 0.01% Tween-20). The PCR procedure comprised an initial denaturation for 10 min at  $95^{\circ}\text{C}$ , followed by 39 cycles of  $92^{\circ}\text{C}$  for 30 s and  $53^{\circ}\text{C}$ ,  $57.5^{\circ}\text{C}$ ,  $59^{\circ}\text{C}$ ,  $61^{\circ}\text{C}$ ,  $63^{\circ}\text{C}$ , and  $65^{\circ}\text{C}$  for 1 min (for rs346158, rs8107914, rs2901077 and rs11666524, rs10104, rs346157, and rs2277947, respectively). Supplementary Figure S1 shows allelic discrimination plots for *C19orf53* assays

designed for this study. Ten percent of the DNA samples were genotyped twice, blinded to the case-control status, in order to assure quality control. Over 99% of the data were concordant.

### 2.3. Statistical and Bioinformatic Analysis

Statistical power was calculated prior to the study using genetic association study power calculator [29]. Association analysis between the *C19orf53* gene polymorphisms and IS risk could detect the genotype relative risk of 1.2–1.4, assuming 0.80 power and 5% type I error ( $\alpha = 0.05$ ) on the sample size of 947 cases and 1308 controls.

The STATISTICA software (v13.3, Santa Clara, California, USA) was utilized for statistical processing. The normality of the distribution for quantitative data was assessed using the Shapiro–Wilk’s test. Given that the majority of quantitative parameters exhibited deviations from normal distribution, they were presented as the median (Me) along with the first and third quartiles [Q1 and Q3]. To compare quantitative variables among two independent groups, the Mann–Whitney test was performed. For categorical variables, differences in statistical significance were evaluated using Pearson’s chi-squared test.

The genotype distributions were assessed for compliance with Hardy–Weinberg equilibrium using Fisher’s exact test. The study groups’ genotype frequencies and their associations with disease risk were analyzed using SNPStats software (<https://www.snpstats.net/start.htm>) (accessed on 23 April 2024). Additive, dominant and recessive models were considered for the genotype association analysis. All calculations were made in relation to the effect allele (EA). The Bonferroni correction was applied additionally to account for multiple comparisons. Associations within the entire group of IS patients/controls were adjusted for age, gender, and smoking status. When information regarding the environmental risk factor was unavailable in the control group, associations were analyzed by comparing the presence or absence of the risk factor in the patient group to the overall control group.

The functional effects of *C19orf53* SNPs were analyzed using the following bioinformatics resources:

- The GTExportal (<http://www.gtexportal.org/> (accessed on 14 May 2024)) was employed to analyze the expression levels of the studied genes in the brain, whole blood, and blood vessels as well as to examine the expression quantitative trait loci (eQTLs) [30].
- For the examination of *C19orf53* SNPs binding to quantitative expression trait loci (eQTL) in peripheral blood, the eQTLGen resource available at <https://www.eqtlgen.org/> (accessed on 14 May 2024) was employed [31].
- HaploReg (v4.2), a bioinformatics tool available at <https://pubs.broadinstitute.org/mammals/haploreg/haploreg.php> (accessed on 14 May 2024), was utilized to assess the associations between *C19orf53* SNPs and specific histone modifications indicative of promoters and enhancers. These modifications included acetylation of lysine residues at positions 27 and 9 of the histone H3 protein as well as mono-methylation at position 4 (H3K4me1) and tri-methylation at position 4 (H3K4me3) of the histone H3 protein. Additionally, the tool was applied to investigate the positioning of SNPs in DNase hypersensitive regions, regulatory motif sites, and locations binding to regulatory proteins [32].
- Bioinformatic tool STRING database (<https://string-db.org/> (accessed on 14 May 2024)) was employed to analyze the primary interaction partners of *C19orf53*. Additionally, the analysis of biological processes and molecular functions related to interactions with key functionally related proteins was conducted using the STRING database [33].
- The mechanisms of interactions between *C19orf53* and cis-eQTL-associated genes were analyzed using the GeneMANIA tool [34].
- The atSNP Function Prediction online tool (<http://atsnp.biostat.wisc.edu/search> (accessed on 15 May 2024)) was utilized to assess how *C19orf53* SNPs affect the gene’s affinity for transcription factors (TFs) based on the presence of reference or alternative



alleles [35]. This tool evaluated the impact of SNPs on TF-DNA interactions using a positional weight matrix to calculate the degree of influence.

- The Gene Ontology online tool (<http://geneontology.org/> (accessed on 15 May 2024)) allowed us to analyze the involvement of transcription factors associated with the reference and SNP alleles in overrepresented biological processes related to IS pathogenesis [36]. This tool helped identify biological functions regulated by TFs linked to *C19orf53* SNPs.
- The Cerebrovascular Disease Knowledge Portal (CDKP) (<https://cd.hugeamp.org/> (accessed on 16 May 2024)) and Cardiovascular Disease Knowledge Portal (<https://cvd.hugeamp.org/> (accessed on 16 May 2024)) integrate and analyze genetic association data from major consortia to study cardio- and cerebrovascular diseases, aiding in the exploration of associations between *C19orf53* SNPs and atherosclerosis-related conditions and risk factors for IS (like low density lipids, body mass index, total cholesterol) [37].

### 3. Results

The *C19orf53* gene is expressed in various parts of the brain as well as in blood vessels and whole blood. *C19orf53* gene expression levels (MeTPM) range from 68.48 to 140.8 in brain tissues, range from 120.5 to 136.0 in blood vessels, and are 45.11 in whole blood (Supplementary Figure S2).

#### 3.1. *C19orf53* SNPs and the Ischemic Stroke Risk: An Analysis of Associations

The genotype frequencies of rs10104, rs11666524, rs346157, rs346158, rs2901077, rs2277947, and rs8107914 *C19orf53* in study groups are presented in Table S2. In the control group, the genotype frequencies of all studied SNPs corresponded to the Hardy–Weinberg equilibrium ( $p > 0.05$ ).

The analysis of the total sample revealed associations between SNPs and the risk of an IS (Table S2): rs346157 (EA G;  $OR_{(R)} = 1.30$ ; 95%  $CI_{(R)} = 1.03$ – $1.64$ ;  $P_{(R)} = 0.03$ ), rs346158 (EA C;  $OR_{(R)} = 1.46$ ; 95%  $CI_{(R)} = 1.01$ – $2.11$ ;  $P_{(R)} = 0.04$ ), and rs2901077 (EA T;  $OR_{(R)} = 2.49$ ; 95%  $CI_{(R)} = 1.11$ – $5.57$ ;  $P_{(R)} = 0.02$ ). However, these associations were weak and did not remain significant after applying Bonferroni correction for the number of regression models (three) (Table S3).

We analyzed the subgroups depending on smoking status, obesity, fresh fruit and vegetable intake, and physical activity level (Table S4). Our data reveal associations between specific genetic variants and the risk of an IS under the three following different conditions: obesity, low physical activity, and low fruit and vegetable intake (Table 2).

First, in obese patients ( $BMI \geq 30$ ), the risk of an IS increases four SNPs *C19orf53*, with P being significant in both recessive (R) and log-additive models (A): rs10104 (EA G;  $OR_{(R)} = 4.7$ ; 95%  $CI_{(R)} = 2.25$ – $9.82$ ;  $P_{(R)} = 0.0003$  ( $P_{(R) \text{ bonf}} = 0.0009$ ) and  $OR_{(A)} = 1.82$ ; 95%  $CI_{(A)} = 1.22$ – $2.72$ ;  $P_{(A)} = 0.004$  ( $P_{(A) \text{ bonf}} = 0.01$ )), rs11666524 (EA A;  $OR_{(R)} = 3.88$ ; 95%  $CI_{(R)} = 1.88$ – $8.02$ ;  $P_{(R)} = 0.001$  ( $P_{(R) \text{ bonf}} = 0.003$ ) and  $OR_{(A)} = 1.76$ ; 95%  $CI_{(A)} = 1.19$ – $2.6$ ;  $P_{(A)} = 0.006$  ( $P_{(A) \text{ bonf}} = 0.02$ )), rs346158 (EA C;  $OR_{(R)} = 3.73$ ; 95%  $CI_{(R)} = 1.81$ – $7.69$ ;  $P_{(R)} = 0.002$  ( $P_{(R) \text{ bonf}} = 0.006$ ) and  $OR_{(A)} = 1.65$ ; 95%  $CI_{(A)} = 1.11$ – $2.44$ ;  $P_{(A)} = 0.015$  ( $P_{(A) \text{ bonf}} = 0.045$ )), and rs2277947 (EA A;  $OR_{(R)} = 4.11$ ; 95%  $CI_{(R)} = 1.98$ – $8.53$ ;  $P_{(R)} = 0.0008$  ( $P_{(R) \text{ bonf}} = 0.002$ ) and  $OR_{(A)} = 1.82$ ; 95%  $CI_{(A)} = 1.22$ – $2.7$ ;  $P_{(A)} = 0.004$  ( $P_{(A) \text{ bonf}} = 0.01$ )) (Table 2).

**Table 2.** Statistically significant correlations between *C19orf53* SNPs and IS risk determined by BMI, fruit and vegetable intake, and physical activity.

SNP	N	Dominant Model		Recessive Model		Log-Additive Model		N	Dominant Model		Recessive Model		Log-Additive Model	
		OR (95% CI) <sup>1</sup>	P (P <sub>bonf</sub> )	OR (95% CI) <sup>1</sup>	P (P <sub>bonf</sub> )	OR (95% CI) <sup>1</sup>	P (P <sub>bonf</sub> )		OR (95% CI) <sup>1</sup>	P (P <sub>bonf</sub> )	OR (95% CI) <sup>1</sup>	P (P <sub>bonf</sub> )	OR (95% CI) <sup>1</sup>	P (P <sub>bonf</sub> )
BMI ≥ 30														
rs10104 <i>C19orf53</i> (A/G)	1286	1.52 [0.90–2.55]	0.12	<b>4.70</b> [2.25–9.82]	<b>0.0003</b> (0.0009)	<b>1.82</b> [1.22–2.72]	<b>0.004</b> (0.01)	1745	0.94 [0.76–1.16]	0.57 (1.0)	<b>1.60</b> [1.02–2.51]	<b>0.046</b> (1.0)	1.02 [0.86–1.22]	0.79 (1.0)
rs11666524 <i>C19orf53</i> (G/A)	1330	1.54 [0.92–2.58]	0.098	<b>3.88</b> [1.88–8.02]	<b>0.001</b> (0.003)	<b>1.76</b> [1.19–2.60]	<b>0.006</b> (0.02)	1792	0.94 [0.76–1.15]	0.55 (1.0)	<b>1.64</b> [1.09–2.48]	<b>0.02</b> (0.06)	1.04 [0.88–1.23]	0.68 (1.0)
rs346158 <i>C19orf53</i> (T/C)	1301	1.40 [0.84–2.35]	0.2	<b>3.73</b> [1.81–7.69]	<b>0.002</b> (0.006)	<b>1.65</b> [1.11–2.44]	<b>0.015</b> (0.045)	1769	0.90 [0.73–1.11]	0.32 (0.96)	<b>1.60</b> [1.06–2.40]	<b>0.03</b> (0.09)	1.01 [0.85–1.19]	0.94 (1.0)
rs2277947 <i>C19orf53</i> (G/A)	1242	1.60 [0.95–2.70]	0.079	<b>4.11</b> [1.98–8.53]	<b>0.0008</b> (0.002)	<b>1.82</b> [1.22–2.70]	<b>0.004</b> (0.01)	1699	0.98 [0.80–1.21]	0.87 (1.0)	<b>1.60</b> [1.05–2.45]	<b>0.03</b> (0.09)	1.06 [0.90–1.26]	0.48 (1.0)
Low physical activity level (f+)														
rs10104 <i>C19orf53</i> (A/G)	1597	0.86 [0.67–1.09]	0.21 (0.63)	<b>1.91</b> [1.19–3.07]	<b>0.009</b> (0.03)	1.00 [0.82–1.22]	0.99 (2.3)	1774	0.93 [0.76–1.15]	0.5 (1.5)	1.14 [0.71–1.83]	0.6 (1.8)	0.97 [0.81–1.15]	0.7 (2.1)
rs11666524 <i>C19orf53</i> (G/A)	1623	0.85 [0.67–1.08]	0.18 (0.5)	<b>1.80</b> [1.13–2.84]	<b>0.016</b> (0.048)	0.99 [0.81–1.20]	0.91 (2.7)	1798	0.97 [0.79–1.20]	0.79 (2.4)	1.29 [0.83–2.00]	0.26 (0.8)	1.02 [0.86–1.21]	0.84 (2.5)
Normal physical activity level (f–)														
Low fruit/vegetable intake (f+)														
rs11666524 <i>C19orf53</i> (G/A)	1739	0.97 [0.78–1.21]	0.81 (2.4)	<b>1.81</b> [1.20–2.75]	<b>0.006</b> (0.02)	1.08 [0.91–1.29]	0.37 (1.1)	1682	0.86 [0.69–1.09]	0.21 (0.6)	1.13 [0.68–1.86]	0.64 (1.9)	0.92 [0.76–1.11]	0.38 (1.1)
rs346157 <i>C19orf53</i> (A/G)	1752	0.91 [0.73–1.13]	0.4 (1.2)	<b>1.42</b> [1.08–1.86]	<b>0.012</b> (0.036)	1.06 [0.91–1.24]	0.43 (1.3)	1699	1.04 [0.82–1.31]	0.76 (2.3)	1.14 [0.85–1.53]	0.4 (1.2)	1.06 [0.90–1.24]	0.51 (1.5)
rs346158 <i>C19orf53</i> (T/C)	1740	0.96 [0.77–1.19]	0.71 (2.1)	<b>1.93</b> [1.29–2.89]	<b>0.0017</b> (0.005)	1.09 [0.92–1.30]	0.33 (1.0)	1687	0.86 [0.68–1.08]	0.18 (0.5)	1.07 [0.65–1.76]	0.79 (2.4)	0.91 [0.75–1.10]	0.31 (0.9)
rs2277947 <i>C19orf53</i> (G/A)	1668	1.02 [0.82–1.27]	0.86 (2.6)	<b>1.81</b> [1.18–2.76]	<b>0.0074</b> (0.02)	1.12 [0.93–1.33]	0.23 (0.7)	1604	0.90 [0.71–1.14]	0.38 (1.1)	1.24 [0.75–2.04]	0.4 (1.2)	0.96 [0.79–1.17]	0.68 (2.0)

All calculations were based on the minor alleles (effect alleles); <sup>1</sup>—odds ratio and 95% confidence interval; *p*-value; statistically significant differences are marked in bold. Effect alleles (EA) are highlighted.

Second, in subjects with low physical activity, the following genetic variants were discovered to be related to the increased risk of an IS: rs10104 (EA G;  $OR_{(R)} = 1.91$ ; 95%  $CI_{(R)} = 1.19$ – $3.07$ ;  $P_{(R)} = 0.009$  ( $P_{(R) \text{ bonf}} = 0.03$ )) and rs11666524 (EA A;  $OR_{(R)} = 1.8$ ; 95%  $CI_{(R)} = 1.13$ – $2.84$ ;  $P_{(R)} = 0.016$  ( $P_{(R) \text{ bonf}} = 0.048$ )) (Table 2).

Third, under the condition of low fruit and vegetable consumption, the following genetic variants were associated with an increased risk of an IS: rs11666524 (EA A;  $OR_{(R)} = 1.81$ ; 95%  $CI_{(R)} = 1.2$ – $2.75$ ;  $P_{(R)} = 0.006$  ( $P_{(R) \text{ bonf}} = 0.02$ )), rs346157 (EA G;  $OR_{(R)} = 1.42$ ; 95%  $CI_{(R)} = 1.08$ – $1.86$ ;  $P_{(R)} = 0.012$  ( $P_{(R) \text{ bonf}} = 0.036$ )), rs346158 (EA C;  $OR_{(R)} = 1.93$ ; 95%  $CI_{(R)} = 1.29$ – $2.89$ ;  $P_{(R)} = 0.0017$  ( $P_{(R) \text{ bonf}} = 0.005$ )), and rs2277947 (EA A;  $OR_{(R)} = 1.81$ ; 95%  $CI_{(R)} = 1.18$ – $2.76$ ;  $P_{(R)} = 0.0074$  ( $P_{(R) \text{ bonf}} = 0.02$ )) (Table 2).

### 3.2. C19orf53 SNPs and Clinical Parameters

Upon analyzing the clinical characteristics in patients with IS, it was observed that allele G rs346157 was associated with lower APTT in patients with low fruit/vegetable intake ( $p = 0.03$ ); allele A rs2277947 was associated with a higher BMI in patients with low fruit/vegetable intake ( $p = 0.004$ ) and in non-smokers ( $p = 0.01$ ) (Figure 2, Table S5).

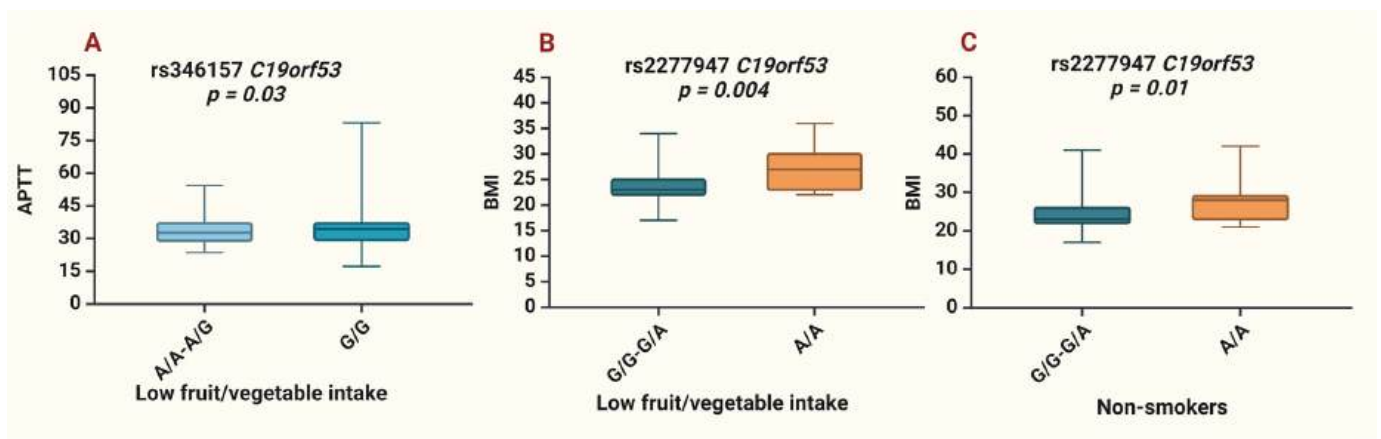


**Figure 2.** Associations of *C19orf53* SNPs and clinical parameter. (A)—APTT values for rs346157 in patients with low fruit and vegetable consumption; (B)—BMI data for rs2277947 in patients with low fruit/vegetable intake; (C)—BMI values for rs2277947 in non-smoking patients.

### 3.3. The Role of Bioinformatic Tools in Substantiating the Results

For the functional annotation of SNPs and the bioinformatic analysis of the role of the *C19orf53* gene in the pathogenetic mechanisms of ischemic stroke, we used a range of tools aimed at analyzing the relationship of SNPs with transcription factors, expression quantitative trait loci, and histone modifications. Additionally, gene–gene and protein–protein interaction networks were constructed.

#### 3.3.1. QTL-Effects

Based on data from the eQTLGene browser SNPs, linked to a higher risk of IS, specifically rs10104 (effect allele G), rs11666524 (effect allele A), rs346158 (effect allele C), and rs2277947 (effect allele A) are associated with reduced levels of expression of both *C19orf53* and *MRI1* as well as increased levels of *CCDC130* and *ZSWIM4* expression in peripheral blood (Table 3). On the other hand, rs346157 (effect allele G) is also linked to reduced expression levels of *C19orf53* and *MRI1* and an increase in *CCDC130* expression but does not affect the expression levels of *ZSWIM4* (Table 3).

GTEx Portal data reveal correlations between IS-associated SNPs and the reduced expression levels of *C19orf53* in brain and adipose tissues as well as in arteries through eQTL effects. Additionally, the expression of the *MRI1* gene shows a decrease in arteries, including the aorta and tibial arteries, as well as in the brain cortex and subcutaneous



adipose tissue. These changes in *MRI1* expression are associated with the presence of rs10104, rs11666524, rs346158, and rs2277947 SNPs (Table 4).

**Table 3.** Relationship between *C19orf53* SNPs and cis-eQTL-mediated expression levels of genes in whole blood (according to browser eQTLGene) (<https://www.eqtlgen.org/>) (accessed on 14 May 2024).

SNP	Assessed Allele	Other Allele	Gene	<i>p</i> -Value	FDR	Z-Score	N Samples
rs10104 <i>C19orf53</i>							
rs10104	<b>G</b>	A	<i>C19orf53</i>	$3.27 \times 10^{-310}$	0	−46.0132	27007
rs10104	<b>G</b>	A	<i>MRI1</i>	$3.27 \times 10^{-310}$	0	−38.6135	26793
rs10104	<b>G</b>	A	<i>CCDC130</i>	$1.10 \times 10^{-19}$	0	9.0787	27007
rs10104	<b>G</b>	A	<i>ZSWIM4</i>	$8.02 \times 10^{-11}$	0	6.5002	21718
rs11666524 <i>C19orf53</i>							
rs11666524	<b>A</b>	G	<i>C19orf53</i>	$3.27 \times 10^{-310}$	0	−46.2734	27279
rs11666524	<b>A</b>	G	<i>MRI1</i>	$3.27 \times 10^{-310}$	0	−39.214	27065
rs11666524	<b>A</b>	G	<i>CCDC130</i>	$6.37 \times 10^{-20}$	0	9.1379	27279
rs11666524	<b>A</b>	G	<i>ZSWIM4</i>	$5.99 \times 10^{-11}$	0	6.5441	21990
rs346157 <i>C19orf53</i>							
rs346157	<b>G</b>	A	<i>C19orf53</i>	$2.14 \times 10^{-214}$	0	−31.2513	27274
rs346157	<b>G</b>	A	<i>MRI1</i>	$9.14 \times 10^{-150}$	0	−26.0647	27060
rs346157	<b>G</b>	A	<i>CCDC130</i>	$2.22 \times 10^{-36}$	0	12.5961	27274
rs346158 <i>C19orf53</i>							
rs346158	<b>C</b>	T	<i>C19orf53</i>	$3.27 \times 10^{-310}$	0	−44.6143	26890
rs346158	<b>C</b>	T	<i>MRI1</i>	$3.27 \times 10^{-310}$	0	−38.1044	26676
rs346158	<b>C</b>	T	<i>CCDC130</i>	$9.10 \times 10^{-18}$	0	8.5849	26890
rs346158	<b>C</b>	T	<i>ZSWIM4</i>	$3.91 \times 10^{-11}$	0	6.6077	21601
rs2277947 <i>C19orf53</i>							
rs2277947	<b>A</b>	G	<i>C19orf53</i>	$3.27 \times 10^{-310}$	0	−46.393	27395
rs2277947	<b>A</b>	G	<i>MRI1</i>	$3.27 \times 10^{-310}$	0	−39.1083	27181
rs2277947	<b>A</b>	G	<i>CCDC130</i>	$5.30 \times 10^{-20}$	0	9.1579	27395
rs2277947	<b>A</b>	G	<i>ZSWIM4</i>	$3.56 \times 10^{-11}$	0	6.6213	22106

Effect allele are marked in bold.

**Table 4.** The impact of SNPs in genes encoding *C19orf53*, gene expression (cis-eQTL) in blood vessels, and brain and blood cells (according to the GTEx Portal browser, <https://gtexportal.org>) (accessed on 14 May 2024).

SNP	GTEx Portal Data ( <a href="https://gtexportal.org">https://gtexportal.org</a> )		
	Gene Expressed	<i>p</i> -Value	Effect (NES)
	<i>C19orf53</i>	$2.7 \times 10^{-18}$	↓ (−0.23)
	<i>MRI1</i>	$3.0 \times 10^{-5}$	↓ (−0.27)
	<i>C19orf53</i>	$8.9 \times 10^{-18}$	↓ (−0.17)
	<i>MRI1</i>	$1.0 \times 10^{-5}$	↓ (−0.23)

Table 4. Cont.

SNP	GTEx Portal Data ( <a href="https://gtexportal.org">https://gtexportal.org</a> )			
	Gene Expressed	<i>p</i> -Value	Effect (NES)	Tissue
rs10104 <i>C19orf53</i> (A/G)	<i>C19orf53</i>	$2.7 \times 10^{-18}$	↓ (−0.23)	Artery—Aorta
	<i>MRI1</i>	$3.0 \times 10^{-5}$	↓ (−0.27)	Artery—Aorta
	<i>C19orf53</i>	$8.9 \times 10^{-18}$	↓ (−0.17)	Artery—Tibial
	<i>MRI1</i>	$1.0 \times 10^{-5}$	↓ (−0.23)	Artery—Tibial
	<i>C19orf53</i>	$9.4 \times 10^{-7}$	↓ (−0.33)	Brain—Amygdala
	<i>C19orf53</i>	$5.1 \times 10^{-8}$	↓ (−0.34)	Brain—Anterior cingulate cortex (BA24)
	<i>C19orf53</i>	$2.5 \times 10^{-18}$	↓ (−0.36)	Brain—Caudate (basal ganglia)
	<i>C19orf53</i>	$2.8 \times 10^{-6}$	↓ (−0.27)	Brain—Cerebellum
	<i>C19orf53</i>	$4.9 \times 10^{-15}$	↓ (−0.42)	Brain—Cortex
	<i>MRI1</i>	$1.7 \times 10^{-5}$	↓ (−0.39)	Brain—Cortex
	<i>C19orf53</i>	$1.2 \times 10^{-15}$	↓ (−0.38)	Brain—Frontal Cortex (BA9)
	<i>C19orf53</i>	$6.2 \times 10^{-12}$	↓ (−0.31)	Brain—Hippocampus
	<i>C19orf53</i>	$3.6 \times 10^{-7}$	↓ (−0.24)	Brain—Hypothalamus
	<i>C19orf53</i>	$3.0 \times 10^{-15}$	↓ (−0.33)	Brain—Nucleus accumbens (basal ganglia)
	<i>C19orf53</i>	$1.3 \times 10^{-8}$	↓ (−0.3)	Brain—Putamen (basal ganglia)
	<i>C19orf53</i>	$6.4 \times 10^{-12}$	↓ (−0.29)	Pituitary
	<i>C19orf53</i>	$2.5 \times 10^{-11}$	↓ (−0.15)	Adipose—Subcutaneous
	<i>MRI1</i>	$9.1 \times 10^{-6}$	↓ (−0.21)	Adipose—Subcutaneous
	<i>C19orf53</i>	$2.3 \times 10^{-9}$	↓ (−0.15)	Adipose—Visceral (Omentum)
	rs11666524 <i>C19orf53</i> (G/A)	<i>C19orf53</i>	$5.5 \times 10^{-18}$	↓ (−0.23)
<i>MRI1</i>		$2.1 \times 10^{-5}$	↓ (−0.27)	Artery—Aorta
<i>C19orf53</i>		$1.7 \times 10^{-17}$	↓ (−0.17)	Artery—Tibial
<i>MRI1</i>		$9.3 \times 10^{-6}$	↓ (−0.23)	Artery—Tibial
<i>C19orf53</i>		$9.3 \times 10^{-7}$	↓ (−0.33)	Brain—Amygdala
<i>C19orf53</i>		$5.6 \times 10^{-8}$	↓ (−0.34)	Brain—Anterior cingulate cortex (BA24)
<i>C19orf53</i>		$7.8 \times 10^{-19}$	↓ (−0.36)	Brain—Caudate (basal ganglia)
<i>C19orf53</i>		$2.7 \times 10^{-6}$	↓ (−0.27)	Brain—Cerebellum
<i>C19orf53</i>		$8.7 \times 10^{-16}$	↓ (−0.42)	Brain—Cortex
<i>MRI1</i>		$2.8 \times 10^{-5}$	↓ (−0.38)	Brain—Cortex
<i>C19orf53</i>		$1.0 \times 10^{-15}$	↓ (−0.37)	Brain—Frontal Cortex (BA9)
<i>C19orf53</i>		$1.4 \times 10^{-10}$	↓ (−0.3)	Brain—Hippocampus
<i>C19orf53</i>	$4.3 \times 10^{-7}$	↓ (−0.23)	Brain—Hypothalamus	
<i>C19orf53</i>	$1.9 \times 10^{-14}$	↓ (−0.32)	Brain—Nucleus accumbens (basal ganglia)	

Table 4. Cont.

SNP	GTEx Portal Data ( <a href="https://gtexportal.org">https://gtexportal.org</a> )			
	Gene Expressed	<i>p</i> -Value	Effect (NES)	Tissue
rs346157 <i>C19orf53</i> (A/G)	<i>C19orf53</i>	$8.6 \times 10^{-9}$	↓ (−0.3)	Brain—Putamen (basal ganglia)
	<i>C19orf53</i>	$8.5 \times 10^{-12}$	↓ (−0.29)	Pituitary
	<i>C19orf53</i>	$1.6 \times 10^{-11}$	↓ (−0.16)	Adipose—Subcutaneous
	<i>MRI1</i>	$6.1 \times 10^{-6}$	↓ (−0.21)	Adipose—Subcutaneous
	<i>C19orf53</i>	$5.1 \times 10^{-9}$	↓ (−0.14)	Adipose—Visceral (Omentum)
	<i>C19orf53</i>	$6.2 \times 10^{-10}$	↓ (−0.15)	Artery—Aorta
	<i>C19orf53</i>	$3.2 \times 10^{-10}$	↓ (−0.11)	Artery—Tibial
	<i>C19orf53</i>	$2.1 \times 10^{-7}$	↓ (−0.27)	Brain—Cortex
	<i>C19orf53</i>	$3.9 \times 10^{-6}$	↓ (−0.22)	Brain—Frontal Cortex (BA9)
	<i>C19orf53</i>	$2.5 \times 10^{-5}$	↓ (−0.17)	Brain—Nucleus accumbens (basal ganglia)
	<i>C19orf53</i>	$5.9 \times 10^{-8}$	↓ (−0.2)	Pituitary
	<i>C19orf53</i>	$9.6 \times 10^{-8}$	↓ (−0.11)	Adipose—Subcutaneous
	<i>C19orf53</i>	$9.5 \times 10^{-14}$	↓ (−0.19)	Artery—Aorta
	<i>MRI1</i>	$6.3 \times 10^{-5}$	↓ (−0.25)	Artery—Aorta
	rs346158 <i>C19orf53</i> (T/C)	<i>C19orf53</i>	$4.1 \times 10^{-13}$	↓ (−0.14)
<i>MRI1</i>		$5.2 \times 10^{-5}$	↓ (−0.2)	Artery—Tibial
<i>C19orf53</i>		$1.1 \times 10^{-5}$	↓ (−0.3)	Brain—Amygdala
<i>C19orf53</i>		$1.7 \times 10^{-7}$	↓ (−0.32)	Brain—Anterior cingulate cortex (BA24)
<i>C19orf53</i>		$2.8 \times 10^{-13}$	↓ (−0.31)	Brain—Caudate (basal ganglia)
<i>C19orf53</i>		$5.0 \times 10^{-10}$	↓ (−0.36)	Brain—Cortex
<i>MRI1</i>		$8.9 \times 10^{-7}$	↓ (−0.47)	Brain—Cortex
<i>C19orf53</i>		$3.2 \times 10^{-15}$	↓ (−0.38)	Brain—Frontal Cortex (BA9)
<i>C19orf53</i>		$3.8 \times 10^{-8}$	↓ (−0.26)	Brain—Hippocampus
<i>C19orf53</i>		$7.8 \times 10^{-6}$	↓ (−0.21)	Brain—Hypothalamus
<i>C19orf53</i>		$3.8 \times 10^{-10}$	↓ (−0.28)	Brain—Nucleus accumbens (basal ganglia)
<i>C19orf53</i>		$1.0 \times 10^{-5}$	↓ (−0.25)	Brain—Putamen (basal ganglia)
<i>C19orf53</i>		$8.4 \times 10^{-9}$	↓ (−0.25)	Pituitary
<i>C19orf53</i>		$4.4 \times 10^{-10}$	↓ (−0.14)	Adipose—Subcutaneous
<i>MRI1</i>		$5.9 \times 10^{-7}$	↓ (−0.23)	Adipose—Subcutaneous
<i>C19orf53</i>	$2.4 \times 10^{-7}$	↓ (−0.13)	Adipose—Visceral (Omentum)	
<i>C19orf53</i>	$5.5 \times 10^{-18}$	↓ (−0.23)	Artery—Aorta	
<i>MRI1</i>	$2.1 \times 10^{-5}$	↓ (−0.27)	Artery—Aorta	
<i>C19orf53</i>	$1.7 \times 10^{-17}$	↓ (−0.17)	Artery—Tibial	
<i>MRI1</i>	$9.3 \times 10^{-6}$	↓ (−0.23)	Artery—Tibial	
<i>C19orf53</i>	$9.3 \times 10^{-7}$	↓ (−0.33)	Brain—Amygdala	

Table 4. Cont.

SNP	GTEx Portal Data ( <a href="https://gtexportal.org">https://gtexportal.org</a> )			Tissue
	Gene Expressed	<i>p</i> -Value	Effect (NES)	
rs2277947 <i>C19orf53</i> (G/A)	<i>C19orf53</i>	<b><math>9.9 \times 10^{-8}</math></b>	↓ (−0.34)	Brain—Anterior cingulate cortex (BA24)
	<i>C19orf53</i>	<b><math>5.2 \times 10^{-18}</math></b>	↓ (−0.36)	Brain—Caudate (basal ganglia)
	<i>C19orf53</i>	<b><math>3.0 \times 10^{-6}</math></b>	↓ (−0.27)	Brain—Cerebellum
	<i>C19orf53</i>	<b><math>1.1 \times 10^{-14}</math></b>	↓ (−0.41)	Brain—Cortex
	<i>MRI1</i>	<b><math>1.0 \times 10^{-5}</math></b>	↓ (−0.4)	Brain—Cortex
	<i>C19orf53</i>	<b><math>4.7 \times 10^{-15}</math></b>	↓ (−0.37)	Brain—Frontal Cortex (BA9)
	<i>C19orf53</i>	<b><math>1.4 \times 10^{-10}</math></b>	↓ (−0.3)	Brain—Hippocampus
	<i>C19orf53</i>	<b><math>4.3 \times 10^{-7}</math></b>	↓ (−0.23)	Brain—Hypothalamus
	<i>C19orf53</i>	<b><math>1.9 \times 10^{-14}</math></b>	↓ (−0.32)	Brain—Nucleus accumbens (basal ganglia)
	<i>C19orf53</i>	<b><math>2.4 \times 10^{-8}</math></b>	↓ (−0.3)	Brain—Putamen (basal ganglia)
	<i>C19orf53</i>	<b><math>8.5 \times 10^{-12}</math></b>	↓ (−0.29)	Pituitary
	<i>C19orf53</i>	<b><math>4.8 \times 10^{-11}</math></b>	↓ (−0.15)	Adipose—Subcutaneous
	<i>MRI1</i>	<b><math>5.1 \times 10^{-6}</math></b>	↓ (−0.21)	Adipose—Subcutaneous
	<i>C19orf53</i>	<b><math>6.2 \times 10^{-9}</math></b>	↓ (−0.14)	Adipose—Visceral (Omentum)

Effect alleles are marked in bold.

Using the GeneMania resource, an analysis of interactions between *C19orf53* and cis-eQTL-associated genes was carried out (*MRI1*, *CCDC130*, *ZSWIM4*). It turned out that they interact through 20 related genes and 125 total links, mainly through physical interactions (77.64%), co-expression (8.01%), prediction (5.37%), co-localization (3.63%), genetic interactions (2.87%), pathways (1.88%), and shared protein domains (0.60%) (Figure 3, Table S6).

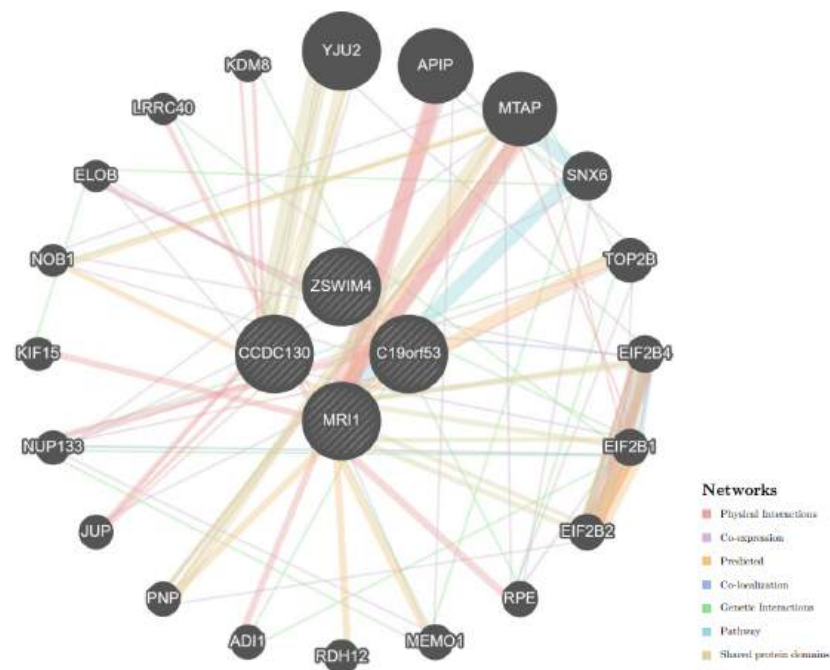


Figure 3. Interactions between *C19orf53* and cis-eQTL-associated genes (24 total genes, 4 searched genes, 20 related genes, 125 total links). Note: Genes searched are indicated with stripes.





Table 5. Cont.

SNP (Ref/Alt Allele)	Tissue Marks	Brain Regions							Peripheral Blood	Adipose
		(1)	(2)	(3)	(4)	(5)	(6)	(7)	(8)	(9)
rs346158 <i>C19orf53</i> (T/C)	H3K4me1	-	-	Enh	-	-	Enh	Enh	Enh	-
	H3K4me3	-	-	-	-	-	-	-	Pro	Pro
	H3K27ac	Enh	Enh	Enh	Enh	Enh	-	Enh	Enh	Enh
	H3K9ac	-	Pro	-	Pro	-	-	-	Pro	-
	DNase	-	-	-	-	-	-	-	-	-
rs2277947 <i>C19orf53</i> (G/A)	H3K4me1	Enh	Enh	Enh	Enh	Enh	-	Enh	Enh	Enh
	H3K4me3	-	-	-	-	-	-	-	Pro	Pro
	H3K27ac	-	-	-	-	-	-	-	Enh	Enh
	H3K9ac	-	-	-	-	-	-	-	Pro	Pro
	DNase	-	-	-	-	-	-	-	-	-

H3K4me1—mono-methylation at the 4th lysine residue of the histone H3 protein; H3K4me3—tri-methylation at the 4th lysine residue of the histone H3 protein; H3K9ac—acetylation at the 9th lysine residues of the histone H3 protein; H3K27ac—acetylation of the lysine residue at N-terminal position 27 of the histone H3 protein; effect alleles are marked in bold. Enh—histone modification associated with gene enhancers; Pro—histone modification associated with gene promoters; 1—Brain (hippocampus); 2—Brain (substantia nigra); 3—Brain (anterior caudate); 4—Brain (cingulate gyrus); 5—Brain (inferior temporal lobe); 6—Brain (angular gyrus); 7—Brain (dorsolateral prefrontal cortex); 8—Any cells from peripheral blood; 9—Adipose Nuclei.

### 3.3.3. Analysis of Transcription Factors

The risk allele G of rs10104 *C19orf53* is associated with the generation of DNA-binding sites for 79 transcription factors (TFs) (Table S8). These TFs are involved in five overrepresented biological processes: the interleukin-9-mediated signaling pathway (GO:0038113; FDR = 0.0245), neuron fate determination (GO:0048664; FDR = 0.0375), the positive regulation of neuron differentiation (GO:0045666; FDR = 0.0105), the regulation of endothelial cell proliferation (GO:0001936; FDR = 0.0353), and the negative regulation of neurogenesis (GO:0050768; FDR = 0.0424) (Table S8).

Nineteen TFs, binding to the risk allele A of rs11666524 *C19orf53*, are concurrently implicated in two overrepresented GO: the positive regulation of neuron differentiation (GO:0045666; FDR = 0.00146) and astrocyte fate commitment (GO:0060018; FDR = 0.00306) (Table S9).

The risk allele G of rs346157 *C19orf53* produces DNA-binding regions for 22 transcription factors, collectively engaged in four overrepresented GOs related to cell proliferation, oxidative stress, cell signaling, and apoptosis: positive regulation of glial cell proliferation (GO:0060252; FDR = 0.0259), cellular response to reactive oxygen species (GO:0034614; FDR = 0.0248), response to hypoxia (GO:0001666; FDR = 0.0197), and mononuclear cell differentiation (GO:1903131; FDR = 0.0371) (Table S10). On the other hand, the protective allele A of rs346157 *C19orf53* provides DNA-binding sites for 63 TFs, which are together participate in 11 GOs associated with the blood vessel morphogenesis (GO:0048514; FDR = 0.00756), regulation of the vascular tone (cellular response to angiotensin (GO:1904385; FDR = 0.00475), neurogenesis (central nervous system development (GO:0007417; FDR = 0.0179)), hypoxia (cellular response to hypoxia (GO:0071456; FDR = 0.00167)), oxidative stress (cellular response to oxidative stress (GO:0034599; FDR = 0.0154)), response to heat (regulation of cellular response to heat (GO:1900034; FDR = 0.0492)), cell signaling (signal transduction by p53 class mediator (GO:0072331; FDR = 0.0071), positive regulation of protein binding (GO:0032092; FDR = 0.00685)), proteostasis (PERK-mediated unfolded protein response (GO:0036499; FDR = 0.015)), and apoptosis (positive regulation of neuron apoptotic process (GO:0043525; FDR = 0.00157), intrinsic apoptotic signaling pathway (GO:0097193; FDR = 0.0462)) (Table S10).

Lastly, the risk allele A of rs2277947 *C19orf53* creates DNA-binding sites for 32 TFs, associated with overrepresented GO such as glial cell fate commitment (GO:0021781;

FDR = 0.0235), the positive regulation of neuron differentiation (GO:0045666; FDR = 0.0341), and blood vessel development (GO:0001568; FDR = 0.0107) (Table S11).

### 3.3.4. Bioinformatic Analysis of the Associations of *C19orf53* SNPs with IS-Related Phenotypes

According to the bioinformatic tools CDKP and CVDKP, the IS-associated *C19orf53* SNPs are linked with ischemic stroke risk and the severity of IS as well as with obesity and a number of laboratory parameters, characterizing the lipid metabolism (Table 6). Particularly noteworthy is the identification of a connection between these SNPs and arterial fibrillation along with indicators of dyslipidemia (triglyceride-to-HDL ratio, serum ApoB),—significant risk factors for IS.

**Table 6.** Results of bioinformatic analyses for *C19orf53* SNPs using Cerebrovascular and Cardiovascular Disease Knowledge Portals.

Tag SNPs	Phenotype	<i>p</i> -Value	Beta (OR)	Sample Size
rs10104 <i>C19orf53</i> (A/G)	<sup>1</sup> All ischemic stroke	0.015	OR▲1.0173	1,047,650
	<sup>1</sup> Modified Rankin scale score 0–2 vs. 3–6 adj stroke severity	0.04	OR▲1.1224	5666
	<sup>2</sup> Atrial fibrillation or flutter	0.014	OR▲1.0291	130,776
	<sup>2</sup> Triglyceride-to-HDL ratio	0.023	Beta▲0.0058	579,558
	<sup>2</sup> Serum ApoB	0.028	Beta▼−0.0048	450,527
rs11666524 <i>C19orf53</i> (G/A)	<sup>1</sup> All ischemic stroke	0.0004	OR▲1.0214	794,817
	<sup>1</sup> Modified Rankin scale score 0–2 vs. 3–6 adj stroke severity	0.029	OR▲1.1324	5666
	<sup>1</sup> Any stroke	0.046	OR▲1.0178	851,850
	<sup>2</sup> Atrial fibrillation or flutter	0.01	OR▲1.0293	130,776
	<sup>2</sup> Triglyceride-to-HDL ratio	0.029	Beta▲0.0075	418,488
	<sup>2</sup> Serum ApoB	0.03	Beta▼−0.0047	436,068
rs346157 <i>C19orf53</i> (A/G)	<sup>1</sup> All ischemic stroke	0.005	OR▲1.0707	38,850
	<sup>1</sup> Cerebral white matter hyperintensity volume	0.033	Beta▲0.0267	11,226
	<sup>2</sup> Dyslipidemia	0.01	OR▲1.0360	56,375
	<sup>2</sup> Obese vs. controls	0.040	OR▲1.0896	4752
rs346158 <i>C19orf53</i> (T/C)	<sup>1</sup> Any stroke	0.006	OR▲1.0870	12,406
	<sup>1</sup> All ischemic stroke	0.003	OR▲1.0202	1,042,380
	<sup>1</sup> Modified Rankin scale score 0–2 vs. 3–6 adj stroke severity	0.012	OR▲1.1511	5666
	<sup>1</sup> Modified Rankin scale score 0–2 vs. 3–6	0.04	OR▲1.1030	5802
	<sup>2</sup> Triglyceride-to-HDL ratio	0.01	Beta▲0.0085	418,488
	<sup>2</sup> Atrial fibrillation or flutter	0.015	OR▲1.0289	130,776
	<sup>2</sup> Serum ApoB	0.04	Beta▼−0.0045	436,068
rs2277947 <i>C19orf53</i> (G/A)	<sup>1</sup> All ischemic stroke	0.005	OR▲1.0193	1,062,920
	<sup>1</sup> Modified Rankin scale score 0–2 vs. 3–6 adj stroke severity	0.03	OR▲1.1308	5666
	<sup>2</sup> Atrial fibrillation or flutter	0.01	OR▲1.0292	130,776
	<sup>2</sup> Triglyceride-to-HDL ratio	0.02	Beta▲0.0079	418,488
	<sup>2</sup> Serum ApoB	0.035	Beta▼−0.0047	436,068

<sup>1</sup>—Cerebrovascular Disease Knowledge Portal data; <sup>2</sup>—Cardiovascular Disease Knowledge Portal data. Effect alleles are marked in bold.

### 3.3.5. Protein–Protein Interactions

Nine proteins having the most prominent interactions with *C19orf53* were found after searching for the primary functional partners of *C19orf53* using the STRING database data (proteins of the first shell of interactors): POLR2J, *C19orf67*, CCDC124, COPS9, NDUFA11, NDUFB7, SERF2, RNF181, *C9orf16* (PPI enrichment *p*-value = 0.00201) (Supplementary Figure S3, Table S13).

Together, *C19orf53* and its main functional partners are involved in six biological processes, reflecting predominantly ATP synthesis (for example: «mitochondrial respiratory chain complex I assembly» (GO:0032981, FDR = 0.0032), «mitochondrial electron transport, NADH to ubiquinone» (GO:0006120, FDR = 0.0121); «proton motive force-driven mitochondrial ATP synthesis» (GO:0042776, FDR = 0.0032)); proteostasis («proteasome-mediated ubiquitin-dependent protein catabolic process» (GO:0043161; FDR = 0.00083)); and metabolic pathways («nucleobase-containing compound biosynthetic process» (GO:0034654; FDR = 0.0038), «nitrogen compound metabolic process» (GO:0006807; FDR = 0.0354)) (Table S14).

## 4. Discussion

Here, providing genetic evidence that SNPs rs10104, rs11666524, rs346157, rs346158, and rs2277947 *C19orf53* are associated with IS risk, we report that *C19orf53* is involved in the pathogenesis of stroke. In particular, BMI, physical activity, and the consumption of fruit and vegetables act as modifiers of the associations of SNPs rs10104, rs11666524, rs346157, rs346158, and rs2277947 (Figure 4).

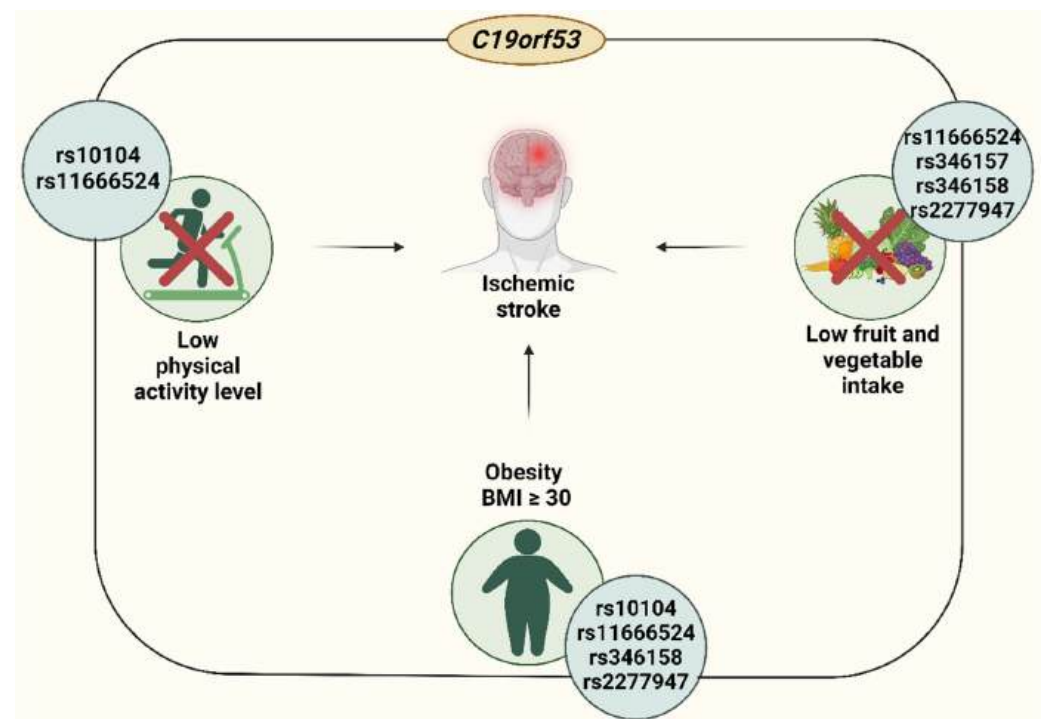


**Figure 4.** The interplay of polymorphic variants of the *C19orf53* gene and environmental factors in the risk of IS development.

Moreover, genotypes A/A-A/G vs. G/G for rs346157 exhibited longer activated partial thromboplastin time (APTT) in patients with insufficient fruit and vegetable intake, and genotypes G/G-G/A vs. A/A for rs2277947 were associated with a higher BMI in non-smokers and patients with low fruit and vegetable intake. Interestingly, another Hero protein member, SERBP1, has also been associated with shorter APTT and a higher BMI [22]. A reduction in APTT, which measures the time required for fibrin formation, is associated

with an elevated risk of ischemic stroke, greater disease severity, and poorer outcomes [38]. Thus, rs346157 may be linked to excessive thrombosis.

SNP rs10104 A/G is a missense variant leading to the substitution of Lys39Arg at codon 39 of the *C19orf53* protein. It is noteworthy that rs10104 is an MRI1 Downstream Variant, significantly affecting the expression of *C19orf53* (Tables 4 and 5). SNPs rs11666524, rs346157, and rs346158 localized in introns, and rs2277947 is a 3' prime UTR variant.

Due to the fact that the use of PubMed and Google Scholar search resources did not allow us to detect studies aimed at investigating the associations of the *C19orf53* SNPs with the development of IS/cardiovascular diseases, we used the bioinformatics analysis to interpret the effects of these genetic variants. Several compelling factors underscore IS-associated SNPs significance in unraveling the mechanisms behind IS.

#### 4.1. *C19orf53* SNPs and the IS Risk: Underlying Mechanisms

Based on cis-eQTL effects and the analysis of transcription factors of *C19orf53* SNPs, associated with IS risk, we distinguished the main mechanisms contributing to disease development (Figure 5).

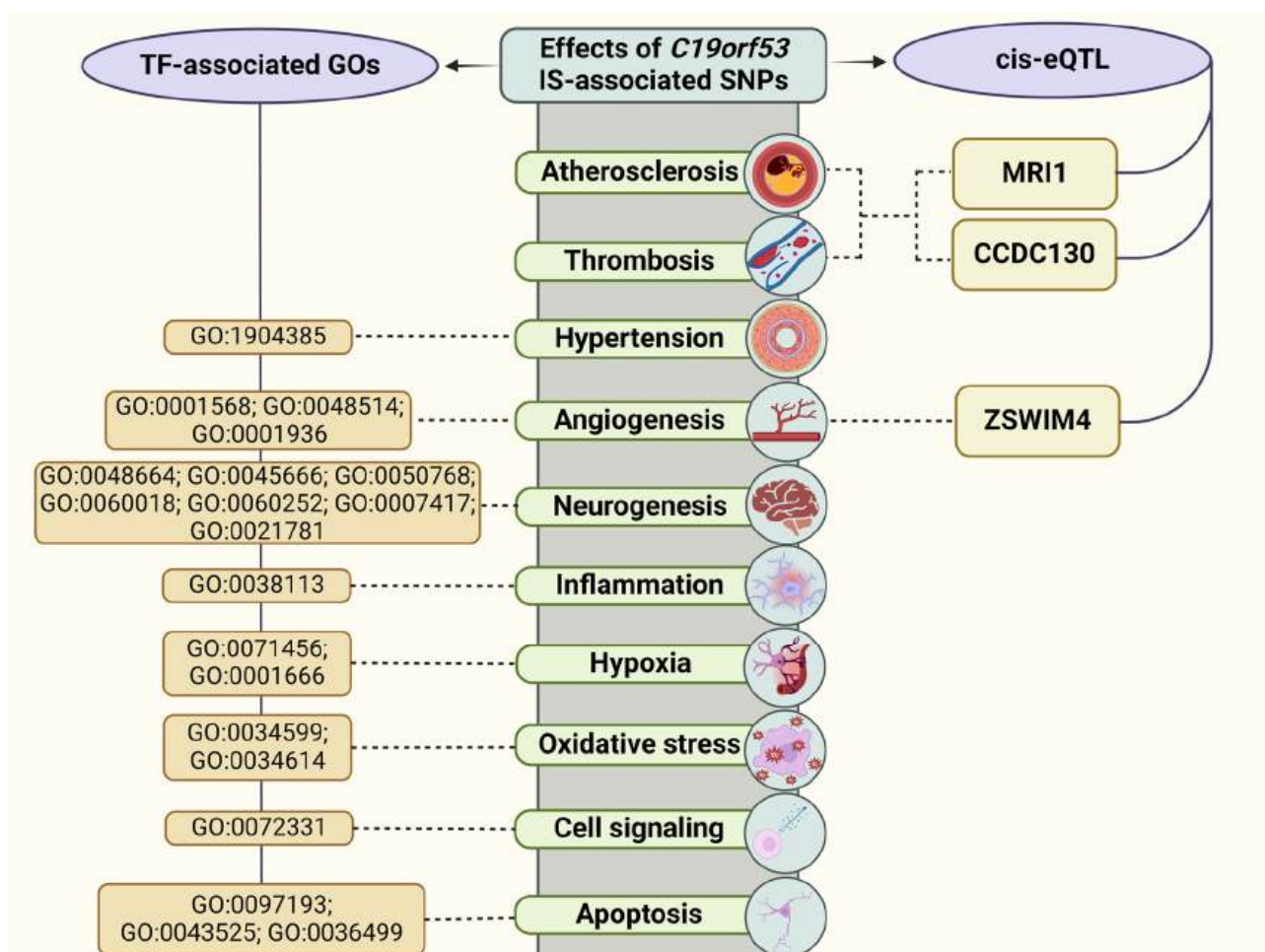


**Figure 5.** The effects of *C19orf53* SNPs associated with IS.

The IS-associated *C19orf53* SNPs exhibit a high level of regulatory potential, exerting profound effects on histone modifications within brain and blood tissues. Notably, they prominently influence histone H3 by inducing trimethylation at the 4th lysine residue, and they also impact the H3K27ac.

Furthermore, it is worth highlighting that the risk alleles of the identified SNPs, which were found to correlate significantly with IS in our study, exhibit associations beyond IS alone,

according to the Cerebrovascular Disease Knowledge Portal. Specifically, these SNPs are associated with an increased risk of all ischemic strokes, as indicated by rs10104, rs11666524, rs346157, rs346158, and rs2277947. Moreover, rs10104, rs11666524, rs346158, and rs2277947 also play a role in determining the severity of stroke, as evidenced by their correlation with modified Rankin scale scores. Additionally, SNPs rs10104, rs11666524, rs346158, and rs2277947 are implicated in atrial fibrillation or flutter, further underscoring their relevance in IS pathogenesis [39]. Complementary, data collected from the Cardiovascular Disease Knowledge Portal reveal that protective alleles of *C19orf53* SNPs exhibit a distinct influence on lipid metabolism, increasing triglyceride to HDL ratio and lowering serum ApoB levels, all of which are critical factors in atherosclerosis and IS development [40].

In ischemic conditions, established molecular mechanisms and cellular processes, including excitotoxicity, oxidative and nitrative stress, inflammation, and apoptosis, contribute to cell death [41]. Recognizing the potential involvement of *C19orf53* polymorphisms in these pathophysiological processes becomes crucial. The IS-associated SNPs of *C19orf53*, which display complex interactions with TFs, are providing insights into their involvement in these important cellular processes. Notably, the risk allele G of rs10104 *C19orf53* generates binding sites for TFs involved in inflammation, neurogenesis, and the regulation of endothelial cell proliferation. Similarly, the risk allele A of rs11666524 *C19orf53* creates binding sites for TFs primarily associated with neuron differentiation and astrocyte fate commitment. Moreover, the risk allele G of rs346157 *C19orf53* provides binding sites for TFs with roles in glial cell proliferation, responses to hypoxia and oxidative stress response, cell signaling, and apoptosis, while its protective A allele introduces binding sites for TFs associated with vasculo- and neurogenesis, the regulation of the vascular tone, hypoxia and oxidative stress response, heat response, cell signaling, proteostasis, and apoptosis. It is worth noting that TFs binding to the DNA site created by protective allele A rs346157 participate in the PERK-mediated pathway. This pathway is involved in protecting the brain from an ischemia–reperfusion injury by inhibiting ER stress-induced apoptosis [42]. Additionally, the risk allele A of rs2277947 *C19orf53* is linked to TFs associated with vasculo- and neurogenesis. In summary, these allele-specific binding sites highlight *C19orf53*'s involvement in pivotal biological processes related to neuron development and differentiation, vasculogenesis, the regulation of vascular tone, and oxidative stress response as well as response to hypoxia, response to heat, proteostasis, inflammation, and the regulation of apoptosis pathways, playing a pivotal role in the molecular pathogenesis of IS [43,44]. Consequently, we can hypothesize that *C19orf53* not only increases the risk of an IS, as established by our genetic analysis, but is also involved in the complex mechanisms governing the survival of neurons, glia, and endothelial cells by means of gains and losses of binding sites for TFs.

To further expand on the involvement of *C19orf53* within cellular functions as well as pathophysiological processes, we analyzed its protein–protein interaction network, shedding light on its principal functional partners and their critical roles. First, *C19orf53* and its principal functional partners participate in processes related to cellular energy production, such as “mitochondrial respiratory chain complex I assembly”, “mitochondrial electron transport, NADH to ubiquinone”, and “proton motive force-driven mitochondrial ATP synthesis”, emphasizing their significance in maintaining energy balance and mitochondrial functionality and potentially in excitotoxicity [45]. Second, their association with “proteasome-mediated ubiquitin-dependent protein catabolic process” signifies a role in maintaining protein homeostasis by aiding in the degradation of damaged proteins [46], a pathway triggered by ischemia [47]. Furthermore, proteins' involvement in “nucleobase-containing compound biosynthetic process” underscores their contributions to nucleotide and nucleic acid metabolism, crucial for DNA and RNA synthesis, ensuring proper cellular function. It is worth noting that *C19orf53* interacts with *C9orf16* and *SERF2*, both correlated with IS risk in our previous studies [20,21]. Collectively, these insights indicate that *C19orf53* and its functional partners are involved in pathophysiological cellular processes, thereby contributing to the underlying mechanisms of IS.



Examining cis-eQTL effects of the IS-associated SNPs, a common theme emerges where these genetic variants (rs10104, rs11666524, rs346157, rs346158, and rs2277947) together contribute to the downregulation of *C19orf53* expression in various tissue types, including blood, brain, and adipose tissues and arteries. Moreover, these SNPs, with the exception of rs346157, exhibit a similar pattern of lowering the expression of the *MRI1* gene in arteries, adipose tissues, and the brain cortex. *MRI1* plays a vital role as an enzyme involved in the methionine de novo and salvage pathway as well as the metabolism of sulfur amino acid (<https://www.genecards.org>, assessed 25 May 2024). We hypothesize that the reduction in *MRI1* production resulting from these SNP-driven alterations may have profound consequences, disrupting these essential metabolic pathways. Notably, the methionine cycle, in which *MRI1* plays a role, holds significant importance in stroke and cardiovascular diseases through the regulation of homocysteine levels [48]. Additionally, sulfur-containing amino acids and their derivatives can regulate body weight, adipogenesis, lipolysis, and glucose metabolism [49], providing a link to associations between *C19orf53* SNPs and an increased BMI.

In contrast, *ZSWIM4* displays an increased expression in blood affected by the risk alleles of rs10104, rs11666524, rs346158, and rs2277947. Expanding on the role of *ZSWIM4* in the context of IS, it is important to highlight its involvement in the ubiquitination pathway, as demonstrated in studies [50]. Mechanically, *ZSWIM4* has been found to have physical interactions with *Smad1*, leading to the ubiquitination and subsequent degradation of *Smad1* [51]. This interaction holds significance within the broader context of IS, as *Smad1* intersects with the regulation of angiogenesis following ischemia/reperfusion. Specifically, the TGF- $\beta$ 1/ALK1/*Smad1*/5/8 signaling pathway has been identified as a key player in mediating angiogenic processes in response to ischemic events [52,53]. By influencing the ubiquitination and degradation of *Smad1*, the increased expression of *ZSWIM4*, caused by the effects of *C19orf53* SNPs, in blood may contribute to the downregulation of this critical pathway, potentially impacting the post-ischemic angiogenic response. Conversely, the presence of IS-associated alleles of *C19orf53* is associated with higher expression levels of *CCDC130* in blood. This observation is of particular significance since members of the *CCDC* protein family, to which *CCDC130* belongs, have been demonstrated to have roles in lipid metabolism and inflammation [54], atherosclerosis, and thrombus formation [55,56]. This intriguing association suggests a potential link between *C19orf53* and the development of IS through the modulation of *CCDC130* expression and its implications in pathological pathways.

The analysis of the joint functions of genes in a network of interactions of *C19orf53* and cis-eQTL-related genes showed that their participation in such processes was significant for the development of IS as oligodendrocyte differentiation, a sulfur amino acid metabolic process. Researchers have already shown the significant role of sulfur amino acids in atherosclerosis [57], and it was found that sulfur-containing amino acid metabolites are associated with the risk of ischemic stroke and fibrin clot properties [58,59] and affect the concentration of glutathione [60], a powerful antioxidant, the level of which can largely determine the risk of an IS [61]. Moreover, plasma sulfur amino acids are obesogenic [62].

Additionally, to further emphasize *C19orf53*'s potential impact on the risk of stroke, there exists a significant relationship between *C19orf53* and Heat Shock Factor 1 (*HSF1*) discovered by the authors [16]. Notably, experiments involving *HSF1* knockout demonstrated a substantial reduction in *C19orf53* expression, underscoring the regulatory influence of *HSF1* on *C19orf53*. *HSF1*, known as a heat shock factor, plays a pivotal role in orchestrating stress-induced transcription and governing diverse physiological processes within cells. Its central position in maintaining cellular homeostasis is well-established, primarily through its ability to transactivate genes responsible for encoding heat shock proteins (HSPs). This newfound association underscores the implication of *C19orf53* in the heat stress response, a pathway of paramount importance in the context of ischemia/reperfusion events and stroke pathogenesis.

#### 4.2. Insufficient Fruit and Vegetable Intake-Linked Associations of *C19orf53*

The correlation of SNPs rs10104, rs11666524, rs346157, rs346158, and rs2277947 with IS was significantly modified by the levels of fresh vegetable and fruit consumption. The link between a reduced intake of fresh vegetables and fruits and increased oxidative stress has been well established. Oxidative stress has been extensively studied and demonstrated to play a significant role in the risk of IS and related phenotypes in numerous investigations. Plant-rich diets, typically rich in phenolic acids, flavonoids, and carotenoids, are known for their potent antioxidant properties. These antioxidants effectively combat excessive reactive oxygen species in the body, safeguarding cells from their negative effect and consequently lowering the risk of cardiovascular diseases.

The analysis of transcriptomic profiling data has unveiled a significant correlation between *C19orf53* and key genes involved in oxidative stress response, shedding light on its potential role in the risk of stroke. Notably, *C19orf53* exhibits strong correlations with *PARK7*, *SOD1*, and *ROCK1*, all playing a crucial part in autophagic proteolysis and autophagosome formation [63–65]. *PARK7*, in particular, is reported as a multifaceted player in the cellular defense against oxidative stress. Acting as a redox-sensitive chaperone and an oxidative stress sensor, *PARK7* is instrumental in safeguarding neurons against oxidative stress-induced cells. Moreover, it prevents the formation of advanced glycation end-products, eliminates hydrogen peroxide, and maintains proper mitochondrial functions, including the autophagy of dysfunctional mitochondria. Additionally, *PARK7* regulates inflammatory responses in astrocytes and neuronal cells. *SOD1*, another gene strongly correlated with *C19orf53*, plays a key role in antioxidant defense [66]. Its protein product is a scavenger of harmful superoxide radicals by converting them into molecular oxygen and hydrogen peroxide. Lastly, *ROCK1*, while not directly involved in oxidative stress response, acts as a negative regulator of VEGF-induced angiogenic endothelial cell activation, which can have implications in vascular health and stroke risk. This intricate web of correlations underscores the potential involvement of *C19orf53* in oxidative stress pathways and its connection to the risk of stroke.

#### 4.3. Low Physical Activity-Related Correlates of *C19orf53*

Numerous studies have consistently demonstrated the benefits of physical exercise, establishing a positive connection to better heart and vessel health [67]. Exercising increases the expression levels of HSPs [68] as well as HSF1 [69]. As previously mentioned, *HSF1* regulates the expression of *C19orf53*. The upregulation of *C19orf53* levels can yield positive effects, as it participates in stress responses, leading to antioxidant [70] and anti-inflammatory effects [71,72] in brain tissues. Another protein linked to *C19orf53*, as discussed earlier, is VEGF. The expression of *VEGF* increases in response to exercise [73–77]. VEGF is significant for neurovascular integrity, participating in endothelial cell proliferation and angiogenesis and in securing neurotrophic, neuroprotective, and neurogenic effects [78]. The interplay of exercise-induced molecular responses involving HSPs, HSF1, *C19orf53*, and VEGF results in an increased risk of an IS for patients with low physical activity levels carrying rs10104 and rs11666524 *C19orf53* SNPs.

#### 4.4. Obesity-Related Correlates of *C19orf53*

Obesity had a substantial impact on the relationship between rs11666524, rs346158, and rs2277947 and the risk of an IS. Patients with a BMI of 30 or greater exhibited significant associations. The Bonferroni adjustment leveled associations in the subgroup with BMI < 30, except for rs10104 *C19orf53*, which maintained a weak connection at  $p = 0.046$ . First, overweight and obesity have been associated with a gradually greater risk of stroke, as revealed by a vast amount of research [79–81]. A bioinformatics study of PheWAS, carried out with the support of Knowledge Portals resources, indicated the influence of all IS-related SNPs on the abdominal fat ratio; rs346157 also exhibited a substantial risk effect in the phenotype “obese vs. controls” (Table 6). Furthermore, our research shows that these SNPs have significant cis-eQTL-mediated effects on both *C19orf53* and *MRI1* expression

levels. MRI1 has been found to alter the metabolism of sulfur-containing amino acids and their derivatives, which play important roles in body weight regulation, adipogenesis, lipolysis, and glucose metabolism [49], implying a relationship between the *C19orf53* SNPs and an increased BMI. Additionally, the assessment of SNPs' histone modifications shows that obesity-related SNPs are characterized by high levels of epigenetic modulation in adipose tissue. Further studies of *C19orf53* SNPs are required, primarily to analyze their associations with the risk of obesity and BMI, which will allow us to determine whether IS-related *C19orf53* SNPs are characterized by pronounced horizontal pleiotropic effects on the development of both IS and obesity or whether their effect on IS is due to mediators' effects, reflecting their influence on the risk of IS through excess body weight.

## 5. Conclusions

The present study provides genetic evidence of associations between *C19orf53* polymorphisms and IS in the Caucasian population of central Russia. The results were supported with a bioinformatic assessment, revealing genome-, epigenome-, and proteome-wide effects of *C19orf53* polymorphisms as well as an established link between SNPs in the *C19orf53* gene and cerebrovascular disease-related phenotypes.

## 6. Limitations of the Study

Our study has several limitations. First, we did not study the level of *C19orf53* expression, which does not allow us to establish the effect of the studied SNPs on the level of *C19orf53* mRNA. Second, we were limited in our analysis of environmental risk factor scores, especially in the control group, which did not allow us to conduct a model-based multifactor dimensionality reduction (MDR) analysis of gene–environment interactions. Third, we did not replicate our data in another independent population sample.

**Supplementary Materials:** The following supporting information can be downloaded at <https://www.mdpi.com/article/10.3390/life14091158/s1>, Supplementary Figure S1: Allelic discrimination plots for *C19orf53* assays designed for this study. (A) rs10104 *C19orf53*. (B) rs11666524 *C19orf53*. (C) rs346157 *C19orf53*. (D) rs346158 *C19orf53*. (E) rs2277947 *C19orf53*. (F) rs2901077 *C19orf53*. (G) rs8107914 *C19orf53*; Supplementary Figure S2: *C19orf53* expression levels in vessels, brain, and peripheral blood; Supplementary Figure S3: Predicted interaction partners of *C19orf53*; Table S1: Primers and probes designed for the study; Table S2: The analysis of the correspondence of the distribution of *C19orf53* genotypes to the Hardy–Weinberg equilibrium; Table S3: The relationship between *C19orf53* gene SNPs and ischemic stroke risk (entire group); Table S4: Smoking, BMI, fruit and vegetable intake, and physical activity level-depending associations between *C19orf53* SNPs and IS risk; Table S5: Statistically significant correlations between *C19orf53* SNPs and clinical parameter IS patients; Table S6: Mechanisms of interactions between *C19orf53* and cis-eQTL-related genes (results of analysis using the GeneMania resource); Table S7: Biological processes characterizing the joint functions of genes in a network of interactions of *C19orf53* and cis-eQTL-related genes; Table S8: Effects of rs10104 *C19orf53* on the binding of DNA to TFs; Table S9: Effects of rs11666524 *C19orf53* on the binding of DNA to TFs; Table S10: Effects of rs346157 *C19orf53* on the binding of DNA to TFs; Table S11: Effects of rs2277947 *C19orf53* on the binding of DNA to TFs; Table S12: Effects of rs346158 *C19orf53* on the binding of DNA to TFs; Table S13: Basic molecular characteristics of predicted functional partners of *C19orf53*; Table S14: Functional enrichments of *C19orf53* network.

**Author Contributions:** Conceptualization, O.B.; methodology, O.B.; validation, A.D., V.P. and E.P.; formal analysis, I.S. and A.D.; investigation, I.S., V.P. and E.P.; data curation, O.B.; writing—original draft preparation, I.S., K.K. and O.B.; writing—review and editing, I.S. and O.B.; visualization, K.K.; supervision, O.B.; project administration, O.B.; funding acquisition, A.D. and O.B. All authors have read and agreed to the published version of the manuscript.

**Funding:** This study was funded by Russian Science Foundation (N° 22-15-00288, <https://rscf.ru/en/project/22-15-00288/>).

**Institutional Review Board Statement:** The study was conducted according to the guidelines of the Declaration of Helsinki and was approved by the Ethical Review Committee of Kursk State Medical University, Russia (Protocol No. 12, accessed on 7 December 2015). All the participants gave written informed consent before the enrollment in this study.

**Informed Consent Statement:** Informed consent was obtained from all subjects involved in the study.

**Data Availability Statement:** The data presented in this study are available upon request from corresponding author.

**Conflicts of Interest:** The authors declare no conflicts of interest.

## References

- Saini, V.; Guada, L.; Yavagal, D.R. Global Epidemiology of Stroke and Access to Acute Ischemic Stroke Interventions. *Neurology* **2021**, *97*, S6–S16. [[CrossRef](#)] [[PubMed](#)]
- Koyama, R.; Shichita, T. Glial Roles in Sterile Inflammation after Ischemic Stroke. *Neurosci. Res.* **2023**, *187*, 67–71. [[CrossRef](#)] [[PubMed](#)]
- Candelario-Jalil, E.; Dijkhuizen, R.M.; Magnus, T. Neuroinflammation, Stroke, Blood-Brain Barrier Dysfunction, and Imaging Modalities. *Stroke* **2022**, *53*, 1473–1486. [[CrossRef](#)] [[PubMed](#)]
- Giffard, R.G.; Yenari, M.A. Many Mechanisms for Hsp70 Protection From Cerebral Ischemia. *J. Neurosurg. Anesthesiol.* **2004**, *16*, 53. [[CrossRef](#)]
- Kobzeva, K.A.; Soldatova, M.O.; Stetskaya, T.A.; Soldatov, V.O.; Deykin, A.V.; Freidin, M.B.; Bykanova, M.A.; Churnosov, M.I.; Polonikov, A.V.; Bushueva, O.Y. Association between HSPA8 Gene Variants and Ischemic Stroke: A Pilot Study Providing Additional Evidence for the Role of Heat Shock Proteins in Disease Pathogenesis. *Genes* **2023**, *14*, 1171. [[CrossRef](#)]
- Truettner, J.S.; Hu, K.; Liu, C.L.; Dietrich, W.D.; Hu, B. Subcellular Stress Response and Induction of Molecular Chaperones and Folding Proteins after Transient Global Ischemia in Rats. *Brain Res.* **2009**, *1249*, 9–18. [[CrossRef](#)]
- Venediktov, A.A.; Bushueva, O.Y.; Kudryavtseva, V.A.; Kuzmin, E.A.; Moiseeva, A.V.; Baldycheva, A.; Meglinski, I.; Piavchenko, G.A. Closest Horizons of Hsp70 Engagement to Manage Neurodegeneration. *Front. Mol. Neurosci.* **2023**, *16*, 1230436. [[CrossRef](#)]
- Jiang, J.; Cyr, D.; Babbitt, R.W.; Sessa, W.C.; Patterson, C. Chaperone-Dependent Regulation of Endothelial Nitric-Oxide Synthase Intracellular Trafficking by the Co-Chaperone/Ubiquitin Ligase CHIP. *J. Biol. Chem.* **2003**, *278*, 49332–49341. [[CrossRef](#)]
- Bushueva, O.; Solodilova, M.; Ivanov, V.; Polonikov, A. Gender-Specific Protective Effect of the –463G>A Polymorphism of Myeloperoxidase Gene against the Risk of Essential Hypertension in Russians. *J. Am. Soc. Hypertens.* **2015**, *9*, 902–906. [[CrossRef](#)]
- Bushueva, O. Single Nucleotide Polymorphisms in Genes Encoding Xenobiotic Metabolizing Enzymes Are Associated with Predisposition to Arterial Hypertension. *Res. Results Biomed.* **2020**, *6*, 447–456. [[CrossRef](#)]
- Madrigal-Matute, J.; de Bruijn, J.; van Kuijk, K.; Riascos-Bernal, D.F.; Diaz, A.; Tasset, I.; Martín-Segura, A.; Gijbels, M.J.J.; Sander, B.; Kaushik, S.; et al. Protective Role of Chaperone-Mediated Autophagy against Atherosclerosis. *Proc. Natl. Acad. Sci. USA* **2022**, *119*, e2121133119. [[CrossRef](#)] [[PubMed](#)]
- Xu, Q.; Metzler, B.; Jahangiri, M.; Mandal, K. Molecular Chaperones and Heat Shock Proteins in Atherosclerosis. *Am. J. Physiol.-Heart Circ. Physiol.* **2012**, *302*, H506–H514. [[CrossRef](#)] [[PubMed](#)]
- Sorokin, A.; Kotani, K.; Bushueva, O.; Taniguchi, N.; Lazarenko, V. The Cardio-Ankle Vascular Index and Ankle-Brachial Index in Young Russians. *J. Atheroscler. Thromb.* **2015**, *22*, 211–218. [[CrossRef](#)] [[PubMed](#)]
- Staron, M.; Wu, S.; Hong, F.; Stojanovic, A.; Du, X.; Bona, R.; Liu, B.; Li, Z. Heat-Shock Protein Gp96/Grp94 Is an Essential Chaperone for the Platelet Glycoprotein Ib-IX-V Complex. *Blood J. Am. Soc. Hematol.* **2011**, *117*, 7136–7144. [[CrossRef](#)]
- Nosaka, M.; Ishida, Y.; Kuninaka, Y.; Ishigami, A.; Taruya, A.; Shimada, E.; Hashizume, Y.; Yamamoto, H.; Kimura, A.; Furukawa, F. Relationship between Intrathrombotic Appearance of HSP27 and HSP70 and Thrombus Ages in a Murine Model of Deep Vein Thrombosis. *Sci. Rep.* **2023**, *13*, 22416. [[CrossRef](#)]
- Tang, Y.; Liao, S.; Liu, G.; Xiong, X.; Liu, H.; Li, F.; Tan, Z.; Kong, X.; Yin, Y.; Tan, B. Advanced Single-Cell Pooled CRISPR Screening Identifies C19orf53 Required for Cell Proliferation Based on mTORC1 Regulators. *Cell Biol. Toxicol.* **2022**, *38*, 43–68. [[CrossRef](#)]
- Zhang, Q.; Burdette, J.E.; Wang, J.-P. Integrative Network Analysis of TCGA Data for Ovarian Cancer. *BMC Syst. Biol.* **2014**, *8*, 1338. [[CrossRef](#)]
- Kong, W.; Hayashi, T.; Fiches, G.; Xu, Q.; Li, M.Z.; Que, J.; Liu, S.; Zhang, W.; Qi, J.; Santoso, N. Diversified Application of Barcoded PLATO (PLATO-BC) Platform for Identification of Protein Interactions. *Genom. Proteom. Bioinform.* **2019**, *17*, 319–331. [[CrossRef](#)]
- Tsuboyama, K.; Osaki, T.; Matsuura-Suzuki, E.; Kozuka-Hata, H.; Okada, Y.; Oyama, M.; Ikeuchi, Y.; Iwasaki, S.; Tomari, Y. A Widespread Family of Heat-Resistant Obscure (Hero) Proteins Protect against Protein Instability and Aggregation. *PLoS Biol.* **2020**, *18*, e3000632. [[CrossRef](#)] [[PubMed](#)]
- Kobzeva, K.A.; Shilenok, I.V.; Belykh, A.E.; Gurtovoy, D.E.; Bobyleva, L.A. C9orf16 (BBLN) Gene, Encoding a Member of Hero Proteins, Is a Novel Marker in Ischemic Stroke Risk. *Res. Results Biomed.* **2022**, *8*, 278–292. [[CrossRef](#)]



21. Belykh, A.E.; Soldatov, V.O.; Stetskaya, T.A.; Kobzeva, K.A.; Soldatova, M.O.; Polonikov, A.V.; Deykin, A.V.; Churnosov, M.I.; Freidin, M.B.; Bushueva, O.Y. Polymorphism of SERP2, the Gene Encoding a Heat-Resistant Obscure (Hero) Protein with Chaperone Activity, Is a Novel Link in Ischemic Stroke. *IBRO Neurosci. Rep.* **2023**, *14*, 453–461. [[CrossRef](#)] [[PubMed](#)]
22. Shilenok, I.; Kobzeva, K.; Stetskaya, T.; Freidin, M.; Soldatova, M.; Deykin, A.; Soldatov, V.; Churnosov, M.; Polonikov, A.; Bushueva, O. SERPINE1 mRNA Binding Protein 1 Is Associated with Ischemic Stroke Risk: A Comprehensive Molecular–Genetic and Bioinformatics Analysis of SERBP1 SNPs. *Int. J. Mol. Sci.* **2023**, *24*, 8716. [[CrossRef](#)] [[PubMed](#)]
23. Lam, A.Y.W.; Tsuboyama, K.; Tadakuma, H.; Tomari, Y. DNAJA2 and Hero11 Mediate Similar Conformational Extension and Aggregation Suppression of TDP-43. *RNA* **2024**, *8*, rna.080165.124. [[CrossRef](#)] [[PubMed](#)]
24. Stetskaya, T.A.; Kobzeva, K.A.; Zaytsev, S.M.; Shilenok, I.V.; Komkova, G.V.; Goryainova, N.V.; Bushueva, O.Y. HSPD1 Gene Polymorphism Is Associated with an Increased Risk of Ischemic Stroke in Smokers. *Res. Results Biomed.* **2024**, *10*, 175–186. [[CrossRef](#)]
25. Bushueva, O.Y.; Bulgakova, I.V.; Ivanov, V.P.; Polonikov, A.V. Association of Flavin Monooxygenase Gene E158K Polymorphism with Chronic Heart Disease Risk. *Bull. Exp. Biol. Med.* **2015**, *159*, 776–778. [[CrossRef](#)]
26. Vialykh, E.K.; Solidolova, M.A.; Bushueva, O.I.; Bulgakova, I.V.; Polonikov, A.V. [Catalase gene polymorphism is associated with increased risk of cerebral stroke in hypertensive patients]. *Zhurnal Nevrol. Psikiatrii Im. S.S. Korsakova* **2012**, *112*, 3–7.
27. Polonikov, A.; Vialykh, E.; Vasil'eva, O.; Bulgakova, I.; Bushueva, O.; Illig, T.; Solodilova, M. Genetic Variation in Glutathione S-Transferase Genes and Risk of Nonfatal Cerebral Stroke in Patients Suffering from Essential Hypertension. *J. Mol. Neurosci.* **2012**, *47*, 511–513. [[CrossRef](#)]
28. Koressaar, T.; Remm, M. Enhancements and Modifications of Primer Design Program Primer3. *Bioinformatics* **2007**, *23*, 1289–1291. [[CrossRef](#)]
29. Johnson, J.L.; Abecasis, G.R. GAS Power Calculator: Web-Based Power Calculator for Genetic Association Studies. *BioRxiv* **2017**. [[CrossRef](#)]
30. THE GTEX CONSORTIUM. The GTEx Consortium Atlas of Genetic Regulatory Effects across Human Tissues. *Science* **2020**, *369*, 1318–1330. [[CrossRef](#)]
31. Vösa, U.; Claringbould, A.; Westra, H.-J.; Bonder, M.J.; Deelen, P.; Zeng, B.; Kirsten, H.; Saha, A.; Kreuzhuber, R.; Kasela, S. Unraveling the Polygenic Architecture of Complex Traits Using Blood eQTL Metaanalysis. *BioRxiv* **2018**, 447367. [[CrossRef](#)]
32. Ward, L.D.; Kellis, M. HaploReg: A Resource for Exploring Chromatin States, Conservation, and Regulatory Motif Alterations within Sets of Genetically Linked Variants. *Nucleic Acids Res.* **2012**, *40*, D930–D934. [[CrossRef](#)] [[PubMed](#)]
33. von Mering, C.; Jensen, L.J.; Snel, B.; Hooper, S.D.; Krupp, M.; Foglierini, M.; Jouffre, N.; Huynen, M.A.; Bork, P. STRING: Known and Predicted Protein–Protein Associations, Integrated and Transferred across Organisms. *Nucleic Acids Res.* **2005**, *33*, D433–D437. [[CrossRef](#)]
34. Franz, M.; Rodriguez, H.; Lopes, C.; Zuberi, K.; Montojo, J.; Bader, G.D.; Morris, Q. GeneMANIA Update 2018. *Nucleic Acids Res.* **2018**, *46*, W60–W64. [[CrossRef](#)]
35. Shin, S.; Hudson, R.; Harrison, C.; Craven, M.; Keleş, S. atSNP Search: A Web Resource for Statistically Evaluating Influence of Human Genetic Variation on Transcription Factor Binding. *Bioinformatics* **2019**, *35*, 2657–2659. [[CrossRef](#)]
36. Consortium, G.O. The Gene Ontology Resource: 20 Years and Still GOing Strong. *Nucleic Acids Res.* **2019**, *47*, D330–D338. [[CrossRef](#)]
37. Crawford, K.M.; Gallego-Fabrega, C.; Kourkoulis, C.; Miyares, L.; Marini, S.; Flannick, J.; Burt, N.P.; von Grotthuss, M.; Alexander, B.; Costanzo, M.C.; et al. Cerebrovascular Disease Knowledge Portal. *Stroke* **2018**, *49*, 470–475. [[CrossRef](#)]
38. Lin, C.-H.; Kuo, Y.-W.; Kuo, C.-Y.; Huang, Y.-C.; Hsu, C.-Y.; Hsu, H.-L.; Lin, Y.-H.; Wu, C.-Y.; Huang, Y.-C.; Lee, M.; et al. Shortened Activated Partial Thromboplastin Time Is Associated With Acute Ischemic Stroke, Stroke Severity, and Neurological Worsening. *J. Stroke Cerebrovasc. Dis.* **2015**, *24*, 2270–2276. [[CrossRef](#)]
39. Song, M.-S.; Choi, Y.J.; Kim, H.; Nam, M.J.; Lee, C.; Han, K.; Jung, J.-H.; Park, Y.-G.; Kim, D.-H.; Park, J.-H. Relationship between Blood Pressure Levels and Ischemic Stroke, Myocardial Infarction, and Mortality in Very Elderly Patients Taking Antihypertensives: A Nationwide Population-Based Cohort Study. *BMC Geriatr.* **2021**, *21*, 620. [[CrossRef](#)]
40. Hoshino, T.; Ishizuka, K.; Toi, S.; Mizuno, T.; Nishimura, A.; Takahashi, S.; Wako, S.; Kitagawa, K. Atherogenic Dyslipidemia and Residual Vascular Risk After Stroke or Transient Ischemic Attack. *Stroke* **2022**, *53*, 79–86. [[CrossRef](#)]
41. Khoshnam, S.E.; Winlow, W.; Farzaneh, M.; Farbood, Y.; Moghaddam, H.F. Pathogenic Mechanisms following Ischemic Stroke. *Neurol. Sci.* **2017**, *38*, 1167–1186. [[CrossRef](#)] [[PubMed](#)]
42. Hu, Y.-Q.; Chen, W.; Yan, M.-H.; Lai, J.-J.; Tang, N.; Wu, L. Ischemic Preconditioning Protects Brain from Ischemia/Reperfusion Injury by Attenuating Endoplasmic Reticulum Stress-Induced Apoptosis through PERK Pathway. *Eur. Rev. Med. Pharmacol. Sci.* **2017**, *21*, 5736–5744. [[PubMed](#)]
43. Bushueva, O.; Barysheva, E.; Markov, A.; Belykh, A.; Koroleva, I.; Churkin, E.; Polonikov, A.; Ivanov, V.; Nazarenko, M. DNA Hypomethylation of the MPO Gene in Peripheral Blood Leukocytes Is Associated with Cerebral Stroke in the Acute Phase. *J. Mol. Neurosci.* **2021**, *71*, 1914–1932. [[CrossRef](#)]
44. Soldatov, V.O. Hypoxia-Inducible Factor: Basic Biology and Involvement in Cardiovascular Pathology. *Asian J. Pharm. (AJP)* **2018**, *12*. [[CrossRef](#)]
45. Doyle, K.P.; Simon, R.P.; Stenzel-Poore, M.P. Mechanisms of Ischemic Brain Damage. *Neuropharmacology* **2008**, *55*, 310–318. [[CrossRef](#)] [[PubMed](#)]



46. Jariel-Encontre, I.; Bossis, G.; Piechaczyk, M. Ubiquitin-Independent Degradation of Proteins by the Proteasome. *Biochim. Biophys. Acta (BBA)-Rev. Cancer* **2008**, *1786*, 153–177. [[CrossRef](#)]
47. Thiebaut, A.M.; Hedou, E.; Marciniak, S.J.; Vivien, D.; Roussel, B.D. Proteostasis During Cerebral Ischemia. *Front. Neurosci.* **2019**, *13*. [[CrossRef](#)]
48. Guiraud, S.P.; Montoliu, I.; Da Silva, L.; Dayon, L.; Galindo, A.N.; Corthésy, J.; Kussmann, M.; Martin, F.-P. High-Throughput and Simultaneous Quantitative Analysis of Homocysteine–Methionine Cycle Metabolites and Co-Factors in Blood Plasma and Cerebrospinal Fluid by Isotope Dilution LC–MS/MS. *Anal. Bioanal. Chem.* **2017**, *409*, 295–305. [[CrossRef](#)]
49. Zheng, J.; Xiao, H.; Duan, Y.; Song, B.; Zheng, C.; Guo, Q.; Li, F.; Li, T. Roles of Amino Acid Derivatives in the Regulation of Obesity. *Food Funct.* **2021**, *12*, 6214–6225. [[CrossRef](#)]
50. Forde, N.; Duffy, G.B.; McGettigan, P.A.; Browne, J.A.; Mehta, J.P.; Kelly, A.K.; Mansouri-Attia, N.; Sandra, O.; Loftus, B.J.; Crowe, M.A.; et al. Evidence for an Early Endometrial Response to Pregnancy in Cattle: Both Dependent upon and Independent of Interferon Tau. *Physiol. Genom.* **2012**, *44*, 799–810. [[CrossRef](#)]
51. Wang, C.; Liu, Z.; Zeng, Y.; Zhou, L.; Long, Q.; Hassan, I.U.; Zhang, Y.; Qi, X.; Cai, D.; Mao, B.; et al. ZSWIM4 Regulates Embryonic Patterning and BMP Signaling by Promoting Nuclear Smad1 Degradation. *EMBO Rep* **2024**, *25*, 646–671. [[CrossRef](#)] [[PubMed](#)]
52. Du, J.; Yin, G.; Hu, Y.; Shi, S.; Jiang, J.; Song, X.; Zhang, Z.; Wei, Z.; Tang, C.; Lyu, H. Coicis Semen Protects against Focal Cerebral Ischemia-Reperfusion Injury by Inhibiting Oxidative Stress and Promoting Angiogenesis via the TGFβ/ALK1/Smad1/5 Signaling Pathway. *Aging* **2020**, *13*, 877–893. [[CrossRef](#)] [[PubMed](#)]
53. González-Núñez, M.; Muñoz-Félix, J.M.; López-Novoa, J.M. The ALK-1/Smad1 Pathway in Cardiovascular Physiopathology. A New Target for Therapy? *Biochim. Biophys. Acta* **2013**, *1832*, 1492–1510. [[CrossRef](#)] [[PubMed](#)]
54. Azad, A.K.; Chakrabarti, S.; Xu, Z.; Davidge, S.T.; Fu, Y. Coiled-Coil Domain Containing 3 (CCDC3) Represses Tumor Necrosis Factor-α/Nuclear Factor κB-Induced Endothelial Inflammation. *Cell. Signal.* **2014**, *26*, 2793–2800. [[CrossRef](#)]
55. Kobayashi, S.; Fukuhara, A.; Taguchi, T.; Matsuda, M.; Tochino, Y.; Otsuki, M.; Shimomura, I. Identification of a New Secretory Factor, CCDC3/Favine, in Adipocytes and Endothelial Cells. *Biochem. Biophys. Res. Commun.* **2010**, *392*, 29–35. [[CrossRef](#)]
56. Kobayashi, S.; Kita, S.; Okuzaki, D.; Fujishima, Y.; Otsuki, M.; Kato, H.; Nishizawa, Y.; Miyashita, K.; Yokoyama, C.; Fukuhara, A. Favine/CCDC3 Deficiency Accelerated Atherosclerosis and Thrombus Formation Is Associated with Decreased MEF2C-KLF2 Pathway. *iScience* **2022**, *25*, 105252. [[CrossRef](#)]
57. Selhub, J.; Troen, A.M. Sulfur Amino Acids and Atherosclerosis: A Role for Excess Dietary Methionine. *Ann. N. Y. Acad. Sci.* **2016**, *1363*, 18–25. [[CrossRef](#)]
58. Vinknes, K.J.; Refsum, H.; Turner, C.; Khaw, K.-T.; Wareham, N.J.; Forouhi, N.G.; Imamura, F. Plasma Sulfur Amino Acids and Risk of Cerebrovascular Diseases: A Nested Case-Control Study in the EPIC-Norfolk Cohort. *Stroke* **2021**, *52*, 172–180. [[CrossRef](#)]
59. Sikora, M.; Bretes, E.; Perla-Kaján, J.; Utyro, O.; Borowczyk, K.; Piechocka, J.; Głowacki, R.; Wojtasz, I.; Kaźmierski, R.; Jakubowski, H. Homocysteine Thiolactone and Other Sulfur-Containing Amino Acid Metabolites Are Associated with Fibrin Clot Properties and the Risk of Ischemic Stroke. *Sci. Rep.* **2024**, *14*, 11222. [[CrossRef](#)]
60. Paterson, P.G.; Lyon, A.W.; Kamencic, H.; Andersen, L.B.; Juurlink, B.H. Sulfur Amino Acid Deficiency Depresses Brain Glutathione Concentration. *Nutr. Neurosci.* **2001**, *4*, 213–222. [[CrossRef](#)]
61. Solodilova, M.; Drozdova, E.; Azarova, I.; Klysova, E.; Bykanova, M.; Bushueva, O.; Polonikova, A.; Churnosov, M.; Polonikov, A. The Discovery of GGT1 as a Novel Gene for Ischemic Stroke Conferring Protection against Disease Risk in Non-Smokers and Non-Abusers of Alcohol. *J. Stroke Cerebrovasc. Dis.* **2024**, *33*, 107685. [[CrossRef](#)] [[PubMed](#)]
62. Elshorbagy, A.K.; Kozich, V.; Smith, A.D.; Refsum, H. Cysteine and Obesity: Consistency of the Evidence across Epidemiologic, Animal and Cellular Studies. *Curr. Opin. Clin. Nutr. Metab. Care* **2012**, *15*, 49–57. [[CrossRef](#)] [[PubMed](#)]
63. Lee, D.-H.; Kim, D.; Kim, S.T.; Jeong, S.; Kim, J.L.; Shim, S.M.; Heo, A.J.; Song, X.; Guo, Z.S.; Bartlett, D.L. PARK7 Modulates Autophagic Proteolysis through Binding to the N-Terminally Arginylated Form of the Molecular Chaperone HSPA5. *Autophagy* **2018**, *14*, 1870–1885. [[CrossRef](#)] [[PubMed](#)]
64. Rudnick, N.D.; Griffey, C.J.; Guarnieri, P.; Gerbino, V.; Wang, X.; Piersaint, J.A.; Tapia, J.C.; Rich, M.M.; Maniatis, T. Distinct Roles for Motor Neuron Autophagy Early and Late in the SOD1G93A Mouse Model of ALS. *Proc. Natl. Acad. Sci. USA* **2017**, *114*, E8294–E8303. [[CrossRef](#)] [[PubMed](#)]
65. Gurkar, A.U.; Chu, K.; Raj, L.; Bouley, R.; Lee, S.-H.; Kim, Y.-B.; Dunn, S.E.; Mandinova, A.; Lee, S.W. Identification of ROCK1 Kinase as a Critical Regulator of Beclin1-Mediated Autophagy during Metabolic Stress. *Nat. Commun.* **2013**, *4*, 2189. [[CrossRef](#)]
66. Azarova, I.E.; Gureeva, A.V.; Postnikova, M.I.; Makarenko, V.V.; Klysova, E.Y.; Polonikov, A.V. The Link of Single Nucleotide Polymorphism Rs4880 of the SOD2 Gene to the Development of Microvascular Complications of Type 2 Diabetes Mellitus. *Res. Results Biomed.* **2023**, *9*, 461–473.
67. Patel, H.; Alkhawam, H.; Madanieh, R.; Shah, N.; Kosmas, C.E.; Vittorio, T.J. Aerobic vs Anaerobic Exercise Training Effects on the Cardiovascular System. *World J. Cardiol.* **2017**, *9*, 134. [[CrossRef](#)]
68. Szyller, J.; Bil-Lula, I. Heat Shock Proteins in Oxidative Stress and Ischemia/Reperfusion Injury and Benefits from Physical Exercises: A Review to the Current Knowledge. *Oxidative Med. Cell. Longev.* **2021**, *2021*, 6678457. [[CrossRef](#)]
69. Kochanowicz, A.; Sawczyn, S.; Niespodziński, B.; Mieszkowski, J.; Kochanowicz, K.; Żychowska, M. Cellular Stress Response Gene Expression During Upper and Lower Body High Intensity Exercises. *PLoS ONE* **2017**, *12*, e0171247. [[CrossRef](#)]

70. Kalmar, B.; Greensmith, L. Induction of Heat Shock Proteins for Protection against Oxidative Stress. *Adv. Drug Deliv. Rev.* **2009**, *61*, 310–318. [[CrossRef](#)]
71. Yenari, M.A.; Liu, J.; Zheng, Z.; Vexler, Z.S.; Lee, J.E.; Giffard, R.G. Antiapoptotic and Anti-inflammatory Mechanisms of Heat-shock Protein Protection. *Ann. N. Y. Acad. Sci.* **2005**, *1053*, 74–83. [[PubMed](#)]
72. Chen, Y.; Voegeli, T.S.; Liu, P.P.; Noble, E.G.; Currie, R.W. Heat Shock Paradox and a New Role of Heat Shock Proteins and Their Receptors as Anti-Inflammation Targets. *Inflamm. Allergy-Drug Targets (Former. Curr. Drug Targets-Inflamm. Allergy)(Discontin.)* **2007**, *6*, 91–100.
73. Cotman, C.W.; Berchtold, N.C.; Christie, L.-A. Exercise Builds Brain Health: Key Roles of Growth Factor Cascades and Inflammation. *Trends Neurosci.* **2007**, *30*, 464–472. [[CrossRef](#)] [[PubMed](#)]
74. Taylor, J.M.; Montgomery, M.H.; Gregory, E.J.; Berman, N.E. Exercise Preconditioning Improves Traumatic Brain Injury Outcomes. *Brain Res.* **2015**, *1622*, 414–429. [[CrossRef](#)]
75. Carro, E.; Nuñez, A.; Busiguina, S.; Torres-Aleman, I. Circulating Insulin-like Growth Factor I Mediates Effects of Exercise on the Brain. *J. Neurosci.* **2000**, *20*, 2926–2933. [[CrossRef](#)]
76. Zhang, Q.; Zhang, L.; Yang, X.; Wan, Y.; Jia, J. The Effects of Exercise Preconditioning on Cerebral Blood Flow Change and Endothelin-1 Expression after Cerebral Ischemia in Rats. *J. Stroke Cerebrovasc. Dis.* **2014**, *23*, 1696–1702. [[CrossRef](#)]
77. Otsuka, S.; Sakakima, H.; Sumizono, M.; Takada, S.; Terashi, T.; Yoshida, Y. The Neuroprotective Effects of Preconditioning Exercise on Brain Damage and Neurotrophic Factors after Focal Brain Ischemia in Rats. *Behav. Brain Res.* **2016**, *303*, 9–18. [[CrossRef](#)]
78. Pikula, A.; Beiser, A.S.; Chen, T.C.; Preis, S.R.; Vargias, D.; DeCarli, C.; Au, R.; Kelly-Hayes, M.; Kase, C.S.; Wolf, P.A. Serum Brain-Derived Neurotrophic Factor and Vascular Endothelial Growth Factor Levels Are Associated with Risk of Stroke and Vascular Brain Injury: Framingham Study. *Stroke* **2013**, *44*, 2768–2775. [[CrossRef](#)]
79. Strazzullo, P.; D’Elia, L.; Cairella, G.; Garbagnati, F.; Cappuccio, F.P.; Scalfi, L. Excess Body Weight and Incidence of Stroke: Meta-Analysis of Prospective Studies with 2 Million Participants. *Stroke* **2010**, *41*, e418–e426. [[CrossRef](#)]
80. Wang, X.; Huang, Y.; Chen, Y.; Yang, T.; Su, W.; Chen, X.; Yan, F.; Han, L.; Ma, Y. The Relationship between Body Mass Index and Stroke: A Systemic Review and Meta-Analysis. *J. Neurol.* **2022**, *269*, 6279–6289. [[CrossRef](#)]
81. Shiozawa, M.; Kaneko, H.; Itoh, H.; Morita, K.; Okada, A.; Matsuoka, S.; Kiriya, H.; Kamon, T.; Fujiu, K.; Michihata, N.; et al. Association of Body Mass Index with Ischemic and Hemorrhagic Stroke. *Nutrients* **2021**, *13*, 2343. [[CrossRef](#)] [[PubMed](#)]

**Disclaimer/Publisher’s Note:** The statements, opinions and data contained in all publications are solely those of the individual author(s) and contributor(s) and not of MDPI and/or the editor(s). MDPI and/or the editor(s) disclaim responsibility for any injury to people or property resulting from any ideas, methods, instructions or products referred to in the content.